

ИНСТИТУТ ЗА ФИЗИКУ

ПРИМЉЕНО: 03. 07. 2018			
Рад.јед.	б р о ј	Арх.шифра	Прилог
0801	951/1		

Научном већу

Института за физику, Београд

МОЛБА

С обзиром да испуњавам критеријуме прописане од Министарства просвете, науке и технолошког развоја за стицање звања **научни сарадник**, молим научно веће Института за физику у Београду да покрене поступак за мој избор у наведено звање.

У прилогу достављам:

1. Мишљење руководиоца пројекта са предлогом чланова комисије за избор у звање,
2. Стручну биографију,
3. Преглед научне активности,
4. Елементе за квалитативну анализу рада,
5. Елементе за квантитативну анализу рада,
6. Списак објављених радова,
7. Податке о цитираности,
8. Копије објављених радова,
9. Решење о претходном избору у звање.

У Београду

02.07.2018.

Andrej Buñac
Андреј Буњац

**НАУЧНОМ ВЕЋУ
ИНСТИТУТА ЗА ФИЗИКУ
У БЕОГРАДУ**

Предмет: Мишљење руководиоца пројекта за избор др Андреј Буњаца у звање научни сарадник

Др Андреј Буњац запослен је у Лабораторији за физику атомских сударних процеса, Института за физику у Београду и ангажован је на пројекту основних истраживања финансираним од Министарства просвете, науке и технолошког развоја: ОИ 171020 “Физика судара и фото процеса у атомским, (био) молекуларним и нанодимензионим системима”. У оквиру наведеног пројекта ангажован је теми 3. задатак 3.3. *Фотопроцеси у јаким ласерским пољима и атосекундни процеси*. Др Андреј Буњац се бави теоријским истраживањима резонантног динамичког Штарковог помака у јаким ласерским пољима са применама у селективној мултифотонској јонизацији атома натријума, израчунавањем енергијског спектра и расподеле момената импулса фотоелектрона, те истраживањем процеса прекобарјерне јонизације лаких алкалних атома.

Др Андреј Буњац премашује критеријуме прописане Правилником за избор у научна звања Министарства просвете, науке и технолошког развоја, те сам сагласан да Научно веће Института за физику у Београду покрене поступак за избор др Андреј Буњаца у звање **научни сарадник**.

Предлажем да комисију за избор др Андреј Буњаца у звање научни сарадник чине:

1. др Ненад Симоновић, научни саветник, Институт за физику у Београду
2. др Братислав Маринковић, научни саветник, Институт за физику у Београду, и
3. проф. др Горан Попарић, ванредни професор, Физички факултет у Београду.

У Београду,

26.06.2018.

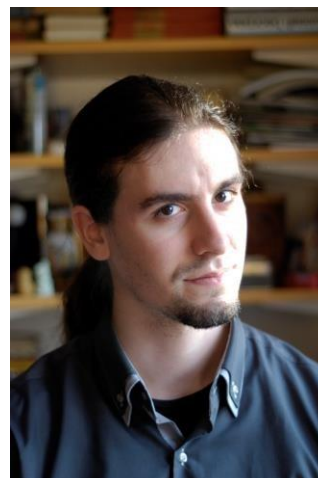
Руководилац пројекта,

Др Братислав Маринковић,
научни саветник

Институт за физику у Београду

Буњац Б. Андреј

Curriculum vitae



Контакт:

E-mail: bunjac@ipb.ac.rs

Лични подаци:

Датум рођења: 03. 12. 1988.

Место рођења: Београд – Савски Венац

Образовање:

2011 – Дипломирао основне студије физике на Физичком факултету у Београду, студијска група: *"Теоријска и експериментална физика"*.

2012 – Дипломирао мастер студије на Физичком факултету у Београду са дипломским радом под називом: *"Модерна теорија поларизације диелектрика"*.

2012 – Уписао докторске студије физике (група *"Квантна, математичка и нанофизика"*) под менторством Др Татјане Вуковић.

2014 – Променио смер докторских студија на *"Физика атома и молекула"* под менторством Др Ненада Симоновића.

2018 – Одбранио докторску дисертацију под називом *"Израчунавање насељености атомских стања, угаоне расподеле и енергијског спектра фотоелектрона код атомских система у јаким ласерским пољима применом временски зависних метода"* под менторством Др Ненада Симоновића.

Професионална ангажованост:

- Новембар 2012 – Новембар 2014: запослен на пројекту *"Карбоснке и неорганске наноструктуре ниске димензионалности"* под руководством Др Милана Дамњановића.
- У летњем семестру 2013/2014 држао експерименталне вежбе из предмета Физика 1 на факултету за физичку хемију.
- Новембар 2014 – сада: запослен на пројекту *"Физика судара и фотопроцеса у атомским, (био)молекулским и нанодимензионим системима"* под руководством Др Братислава Маринковића.
- Септембар 2014 – 2017: изводи наставу математике у *Brook Hill International School* у Београду.
- 2017 – сада: изводи наставу математике у *International School Savremena* у Београду.
- Члан организационог комитета конференције *"COST XLIC WG2 Expert meeting on biomolecules, 27th – 30th April 2015, Fruška Gora"*.

Преглед научне активности кандидата

Кандидат је ангажован на пројекту Министарства просвете, науке и технолошког развоја бр. 171020 и бавио се изучавањем метода решавања временски зависне Шредингерове једначине (методе пропагације таласних пакета) и примене истих на анализу динамике атомских система у јаким пољима.

У том периоду комплетирао је и одбранио своју докторску дисертацију под називом *Израчунавање насељености атомских стања, угаоне расподеле и енергијског спектра фотоелектрона код атомских система у јаким ласерским пољима применом временски зависних метода* под менторством Др Ненада Симоновића и тиме стекао звање доктора наука за физичке науке.

Интеракција атомских и молекулских система са електромагнетним пољем, пре свега са јаким ласерским зрачењем, укључује процесе мултифотонске и тунелне јонизације, затим несеквенцијалне двоструке јонизације, емисије хармоника високог реда, стабилизације атома у електромагнетном пољу, итд.

Конкретни системи које је кандидат испитивао су атоми натријума и литијума у јаким ласерском пољу, изабрани због могућности рачунања у једноелектронској слици (због изузетно захтевних нумеричких процедура). На овим системима испитивани су ефекти јонизације у различитим режимима спољашњег електромагнетног поља, а рачунате су вероватноће јонизације, угаоне расподеле и енергијски спектар фотоелектрона, као и насељености побуђених стања након примењеног ласерског пулса, а све у циљу испитивања ефеката попут резонантно појачане мултифотонске јонизације (*REMPI*), јонизације преко прага (*ATI*), као и рачунања динамичког Штарковог помака. Резултати су објављени у 3 рада у међународним часописима и приказани као 5 саопштења на међународним конференцијама. Такође су били и садржај једног предавања по позиву на међународној конференцији.

1. Рачунање стопе јонизације атома натријума у режиму тунелирања у квазистатичкој апроксимацији

Кандидат је испрограмио нумеричку процедуру за рачунање стопа јонизације и енергија везаних стања код алкалних метала у ласерском пољу велике таласне дужине (око 14 μm) користећи моделни Хелманов потенцијал за опис система. При овако великим таласним дужинама могуће је користити квазистатичку апроксимацију. Кандидат је испитао домен важења квазистатичке апроксимације користећи симулацију реалног пулса за поређење. Показано је да се ова апроксимација може користити у домену у ком је Келдишев параметар $\gamma = \frac{\omega\sqrt{2I_p}}{F}$ мањи од 0.2. Резултати симулација су у добром слагању са објављеним резултатима на сличним системима. Сви добијени резултати приказани су на једној међународној конференцији и објављени у једном раду:

A. Bunjac, D. B. Popović, and N. S. Simonović,

“Wave-packet analysis of strong-field ionization of sodium in the quasistatic regime”,
Eur. Phys. J. D: At. Mol. Clusters & Opt. Phys. **70**(5), 116 (2016). [6 pp]
Topical Issue: Advances in Positron and Electron Scattering, P. Limao -Vieira, G. Garcia,
E. Krishnakumar, J. Sullivan, H. Tanuma and Z. Petrovic (Guest editors)
[DOI: 10.1140/epjd/e2016-60738-0](https://doi.org/10.1140/epjd/e2016-60738-0)
<http://link.springer.com/article/10.1140%2Fepjd%2Fe2016-60738-0>
ISSN: 1434-6060
(Категорија M23)

2. Рачунање угаоних расподела и енергијског спектра фотоелектрона атома натријума и литијума у јаким ласерским пољима.

У оквиру мултифотонског режима нумерички је испитан атом натријума изложен кратким ласерским пулсевима у широком опсегу фреквенција и интензитета поља. Кандидат је опет испрограмирао нумеричку процедуру за еволуцију таласне функције помоћу решавања временски зависне Шредингерове једначине. Као резултат ове симулације дају вероватноће насељености атомских стања и показују услове при којима се одвија резонантно попуњавање. Интерполацијом добијених резултата предложен је метод за рачунање динамичког Штарковог помака под условом резонантности, као и метод за рачунање енергијског спектра фотоелектрона који репродукује профиле добијене услед резонантно појачане мултифотонске јонизације. Добијени резултати упоређени су недавно објављеним експерименталним подацима и дају добро слагање. Поред тога, рачунате су угаоне расподеле фотоелектрона атома натријума и литијума третираних интензивним ласерским пулсевима у трајању неколико десетина фемтосекунди. Из добијених профила импулсном простору израчунати су енергијски спектри који су упоређени са недавно објављеним експерименталним резултатима и дају добро слагање. Ови резултати објављени су у 2 рада:

A. Bunjac, D. B. Popović and N. S. Simonović,
“Resonant dynamic Stark shift as a tool in strong-field quantum control: calculation and application for selective multiphoton ionization of sodium”,
Phys. Chem. Chem. Phys. **19**, 19829-19836 (2017). [on-line 07.07.2017]
<https://doi.org/10.1039/C7CP02146A>
From themed collection XUV/X-ray light and fast ions for ultrafast chemistry
ISSN: 1463-9076
(Категорија M21)

A. Bunjac, D. B. Popović and N. S. Simonović,
“Calculations of photoelectron momentum distributions and energy spectra at strong-field multiphoton ionization of sodium”,
Eur. Phys. J D **71**(8), 208 (2017). [6pp, online 8 Aug.2017]
[doi: 10.1140/epjd/e2017-80276-5](https://doi.org/10.1140/epjd/e2017-80276-5)
Contribution to the Topical Issue: “Physics of Ionized Gases (SPIG 2016)”, Edited by G. Poparic,
B. Obradovic, D. Maric and A. Milosavljevic.
ISSN: 1434-6060
(Категорија M23)

Елементи за квалитативну оцену научног доприноса

1. Квалитет научних резултата

i. Значај научних резултата

Кандидат Андреј Буњац је учествовао у израдањи 3 научна рада и на свима је као први аутор дао кључни допринос. Од тога је један објављен у врхунском међународном часопису категорије M21, а два у међународним часописима категорије M23. Такође, имао је пет саопштења на међународним конференцијама и једно предавање по позиву. Најзначајнији резултати објављени су у следећим радовима:

A. Bunjac, D. B. Popović, and N. S. Simonović,
“Wave-packet analysis of strong-field ionization of sodium in the quasistatic regime”,
Eur. Phys. J. D: At. Mol. Clusters & Opt. Phys. **70**(5), 116 (2016). [6 pp]
Topical Issue: Advances in Positron and Electron Scattering, P. Limao -Vieira, G. Garcia,
E. Krishnakumar, J. Sullivan, H. Tanuma and Z. Petrovic (Guest editors)
[DOI: 10.1140/epjd/e2016-60738-0](https://doi.org/10.1140/epjd/e2016-60738-0)
<http://link.springer.com/article/10.1140%2Fepjd%2Fe2016-60738-0>
ISSN: 1434-6060

A. Bunjac, D. B. Popović and N. S. Simonović,
“Resonant dynamic Stark shift as a tool in strong-field quantum control: calculation and application for selective multiphoton ionization of sodium”,
Phys. Chem. Chem. Phys. **19**, 19829-19836 (2017). [on-line 07.07.2017]
<https://doi.org/10.1039/C7CP02146A>
From themed collection XUV/X-ray light and fast ions for ultrafast chemistry
ISSN: 1463-9076

A. Bunjac, D. B. Popović and N. S. Simonović,
“Calculations of photoelectron momentum distributions and energy spectra at strong-field multiphoton ionization of sodium”,
Eur. Phys. J D **71**(8), 208 (2017). [6pp, online 8 Aug.2017]
[doi: 10.1140/epjd/e2017-80276-5](https://doi.org/10.1140/epjd/e2017-80276-5)
Contribution to the Topical Issue: “Physics of Ionized Gases (SPIG 2016)”, Edited by G. Poparic,
B. Obradovic, D. Maric and A. Milosavljevic.
ISSN: 1434-6060

ii. Параметри квалитета часописа

Кандидат Андреј Буњац је укупно објавио 3 научна рада у међународним часописима и то:

1 рад у врхунском међународном часопису *Physical Chemistry Chemical Physics* (M21, импакт фактор = 4.493, 2017 снп = 1.089)

2 рада у међународном часопису *European Physical Journal D* (M23, импакт фактор = 1.228, 2016 снп = 0.784, 2017 снп = 0.716)

	ИФ	М	СНИП
Укупно	6.949	14	2.521
Усредњено по чланку	2.3163	4.67	0.863
Усредњено по аутору	2.3163	4.67	0.863

iii. Подаци о цитираности

Према бази *Web of Science* радови Андреја Буњца цитирани 1 пут (изузимајући аутоцитате). Према бази *Google Scholar* цитирани су 4 пута од чега 1 изузимајући аутоцитате.

2. Нормирање броја коауторских радова, патената и техничких решења

Сви радови Андреја Буњца имају 3 аутора те се признају са пуним бројем поена. Укупан број поена које је кандидат остварио је 25 што је више од захтеваног минимума (16) за избор у звање научни сарадник.

3. Учешће у пројектима, потпројектима и пројектним задацима

Кандидат је од 1.11.2012. до 31.10.2014. учествовао на пројекту Министарства просвете, науке и технолошког развоја Републике Србије ОИ 171035 "Графитне и неорганске наноструктуре ниске димензионалности". Од 1.11.2014. године ангажован је на пројекту ОИ 171020 "Физика судара и фотопроеца у атомским, (био)молекулским и нанодимензионим системима" Министарства просвете, науке и технолошког развоја Републике Србије, чији руководиоцац је др Братислав Маринковић.

4. Утицај научних резултата

Списак радова и цитата дат је у прилогу.

5. Конкретан допринос кандидата у реализацији радова у научним центрима у земљи и иностранству

Кандидат је све своје научне активности реализовао у Институту за Физику Београд. Значајно је допринео сваком раду у ком је учествовао. Његов допринос је пре свега у креирању нумеричких кодова за опис интеракције валентних електрона алкалних метала (натријума и литијума) са јаким ласерским пољима и реализацији нумеричких прорачуна, а затим и у анализи истих, као и у писању радова.

Елементи за квантитативну оцену научног доприноса

Радови објављени у научним часописима од међународног значаја, научна критика; уређивање часописа (M20):

	број	вредност	укупно
M21	1	8	8
M23	2	3	6

Зборници са међународних научних скупова (M30):

	број	вредност	укупно
M32	1	1.5	1.5
M33	2	1	2
M34	3	0.5	1.5

Одбрањена докторска дисертација (M70):

	број	вредност	укупно
M70	1	6	6

Поређење са захтеваним критеријума од министарства науке:

Научни сарадник	Поени који треба да припадају следећим категоријама	Неопходно	Остварено
Обавезни (1)	M10+M20+M31+M32+M33+M41+M42	10	19
Обавезни (2)	M11+M12+M21+M22+M23	6	14
Укупно	Све категорије	16	25

Буњац Б. Андреј – Списак радова

Радови објављени у научним часописима од међународног значаја, научна критика; уређивање часописа (M20):

(Рад у врхунском међународном часопису - M21):

A. Bunjac, D. B. Popović and N. S. Simonović,

“Resonant dynamic Stark shift as a tool in strong-field quantum control: calculation and application for selective multiphoton ionization of sodium”,

Phys. Chem. Chem. Phys. **19**, 19829-19836 (2017). [on-line 07.07.2017]

<https://doi.org/10.1039/C7CP02146A>

From themed collection XUV/X-ray light and fast ions for ultrafast chemistry
ISSN: 1463-9076

(Рад у међународном часопису - M23):

A. Bunjac, D. B. Popović, and N. S. Simonović,

“Wave-packet analysis of strong-field ionization of sodium in the quasistatic regime”,

Eur. Phys. J. D: At. Mol. Clusters & Opt. Phys. **70**(5), 116 (2016). [6 pp]

Topical Issue: Advances in Positron and Electron Scattering, P. Limao -Vieira, G. Garcia, E. Krishnakumar, J. Sullivan, H. Tanuma and Z. Petrovic (Guest editors)

DOI: [10.1140/epjd/e2016-60738-0](https://doi.org/10.1140/epjd/e2016-60738-0)

<http://link.springer.com/article/10.1140%2Fepjd%2Fe2016-60738-0>

ISSN: 1434-6060

A. Bunjac, D. B. Popović and N. S. Simonović,

“Calculations of photoelectron momentum distributions and energy spectra at strong-field multiphoton ionization of sodium”,

Eur. Phys. J D **71**(8), 208 (2017). [6pp, online 8 Aug.2017]

doi: [10.1140/epjd/e2017-80276-5](https://doi.org/10.1140/epjd/e2017-80276-5)

Contribution to the Topical Issue: “Physics of Ionized Gases (SPIG 2016)”, Edited by G. Poparic, B. Obradovic, D. Maric and A. Milosavljevic.

ISSN: 1434-6060

Зборници са међународних научних скупова (M30):

(Предавање по позиву са међународног скупа штампано у изводу - M32):

A. Bunjac, D. B. Popovic, N. S. Simonovic,

"Calculation of the dynamic Stark shift for sodium and the application to resonantly enhanced multiphoton ionization",

Proc. 7th Conference on Elementary Processes in Atomic Systems (CEPAS 2017), 3rd – 6th September 2017, Průhonice, Czech Republic, Editors: M. Tarana, R. Čurík (J. Heyrovský Institute of Physical Chemistry, Prague, 2017), Abstracts of Oral Contributions, p.13.

ISBN: 978-80-87351-46-8

<https://www.jh-inst.cas.cz/cepas2017/>

(Саопштење са међународног скупа штампано у целини - М33):

A. Bunjac, D. B. Popović and N. S. Simonović,

“Strong-Field Ionization of Sodium in the Quasistatic Regime”,

Proc. 28th Summer School and Int. Symp. on Physics of Ionized Gases – SPIG 2016, August 29th –Sept. 2nd 2016, Belgrade, Serbia, Contributed Papers & Abstracts of Invited Lectures, Topical Invited Lectures, Progress Reports and Workshop Lectures,
Editors: Dragana Marić, Aleksandar R. Milosavljević, Bratislav Obradović, and Goran Poparić, (Univ. of Belgrade, Faculty of Physics and SASA, Belgrade, Serbia), Poster P.1.3, pp.20-23. ISBN: 978-86-84539-14-6.

<http://www.spig2016.ipb.ac.rs/spig2016-book-online.pdf>

A. Bunjac, D. B. Popović and N. S. Simonović,

“Photoionization of Sodium by a Few Femtosecond Laser Pulse - Time-Dependent Analysis”,

Proc. 28th Summer School and Int. Symp. on Physics of Ionized Gases – SPIG 2016, August 29th –Sept. 2nd 2016, Belgrade, Serbia, Contributed Papers & Abstracts of Invited Lectures, Topical Invited Lectures, Progress Reports and Workshop Lectures,
Editors: Dragana Marić, Aleksandar R. Milosavljević, Bratislav Obradović, and Goran Poparić, (Univ. of Belgrade, Faculty of Physics and SASA, Belgrade, Serbia), Poster P.1.2, pp.16-19. ISBN: 978-86-84539-14-6.

<http://www.spig2016.ipb.ac.rs/spig2016-book-online.pdf>

(Саопштење са међународног скупа штампано у изводу - М34):

A. Bunjac D. B. Popović and N. Simonović,

“Calculation of probabilities and photoelectron angular distributions for strong field ionization of sodium”,
3rd General Meeting of XLIC (XUV/X-ray light and fast ions for ultrafast chemistry) COST Action CM1204, 2-4 November 2015 Debrecen, Hungary, Programme and Book of Abstracts, Editor: P. Badankó, Poster presentation, p.29.

<http://xlic.unideb.hu/>

ISBN: 978-963-832-51-0 (Károly Tőkési,, Atomki, Hungary)

A. Bunjac, D. B. Popović, N. Simonović,

“Calculations of ionization probabilities for sodium in strong laser fields”

Proc. WG2 Expert Meeting on Biomolecules, COST Action CM1204, XLIC - XUV/X-ray Light and fast Ions for ultrafast Chemistry, April 27-30, 2015, Book of Abstracts, Eds. Paola Bolognesi and Aleksandar Milosavljević, 27-30 April 2015, Poster presentation P02, p.59.

<http://www.xlic-wg2-2015.ipb.ac.rs/>

ISBN: / (The Institute of Physics, Belgrade, Serbia)

A. Bunjac, D. B. Popović and N. S. Simonović,

“Calculation of populations of energy levels of sodium interacting with an intense laser pulse and estimation of the resonant dynamic Stark shift”,

Proc. The Sixth International School and Conference on Photonics & COST actions: MP1406 and MP1402 & H2020-MSCA-RISE-2015 CARDIALLY workshop (PHOTONICA 2017), 28 August – 1 September 2017 Belgrade, Serbia, Book of abstracts, Abstracts of Tutorial, Keynote, Invited Lectures, Progress Reports and Contributed Papers, Eds. Marina Lekić and Aleksandar Krmpot (Institute of Physics Belgrade, Belgrade, 2017), Section: 9. Laser - material interaction, Contributed Paper L.M.I.10, p.178.

ISBN 978-86-82441-46-5

<http://www.photonica.ac.rs/>

Одбрањена докторска дисертација (M70):

Одбрањена докторска дисертација под називом *Израчунавање насељености атомских стања, угаоне расподеле и енергијског спектра фотоелектрона код атомских система у јаким ласерским пољима* под менторством Др Ненада Симоновића.

Web of Science

Search Search Results

Tools Searches and alerts Search History Marked List

Citation report for 3 results from Web of Science Core Collection between 1996 and 2018 Go

You searched for: AUTHOR: (bunjac) ...More

This report reflects citations to source items indexed within Web of Science Core Collection. Perform a Cited Reference Search to include citations to items not indexed within Web of Science Core Collection.

Export Data: Save to Excel File

Total Publications

3 Analyze

1998 2017

h-index

1

Average citations per item

0.33

Sum of Times Cited

1

Without self citations

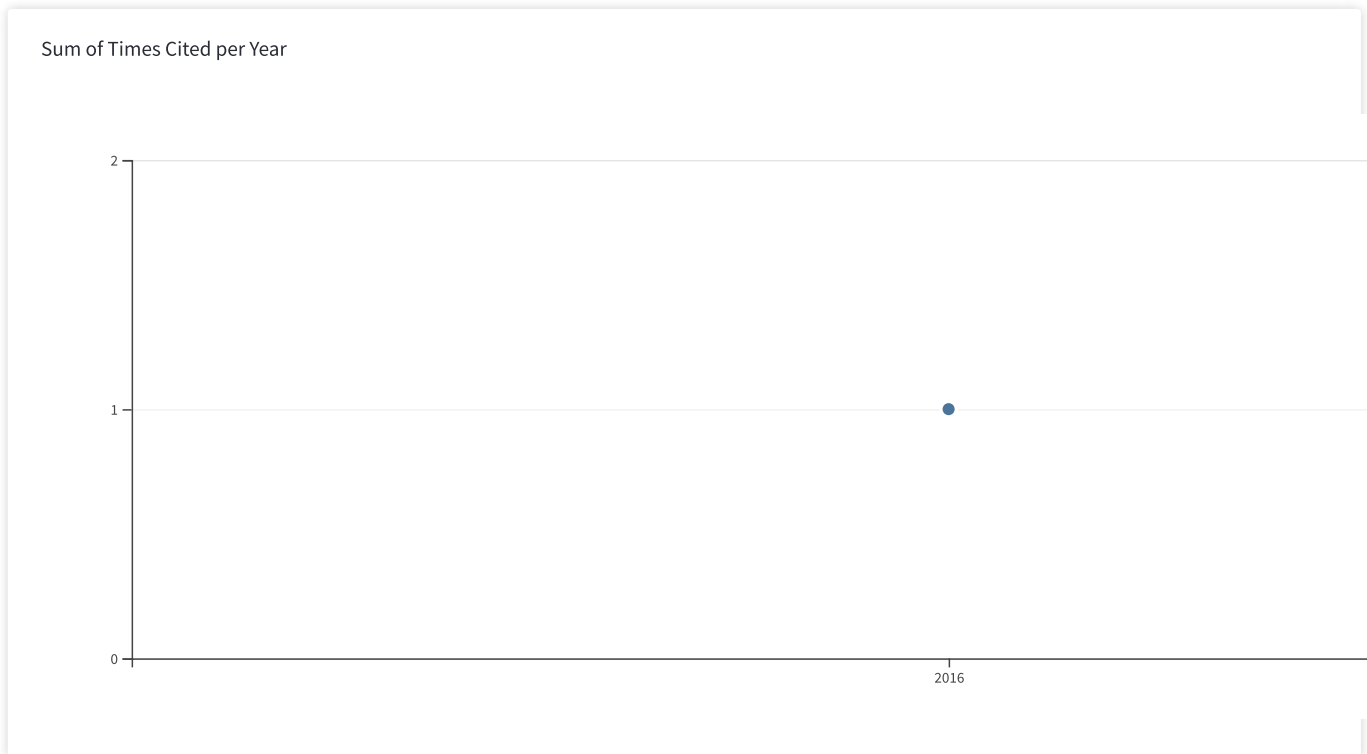
1

Citing articles

1 Analyze

Without self citations

1 Analyze



Sort by: Times Cited Date More

Page 1 of 1

2014	2015	2016	2017	2018	Total	Average Citations per Year
		1			1	0.33

Use the checkboxes to remove individual items from this Citation Report

0 0 1 0 0 1 0.33

or restrict to items published between

and

- 1. **Wave-packet analysis of strong-field ionization of sodium in the quasistatic regime**
By: Bunjac, Andrej; Popovic, Duska B.; Simonovic, Nenad S. 0 0 1 0 0 1 0.33
[EUROPEAN PHYSICAL JOURNAL D](#) Volume: 70 Issue: 5 Article Number: 116
Published: MAY 24 2016

- 2. **Resonant dynamic Stark shift as a tool in strong-field quantum control: calculation and application for selective multiphoton ionization of sodium**
By: Bunjac, A.; Popovic, D. B.; Simonovic, N. S. 0 0 0 0 0 0 0.00
[PHYSICAL CHEMISTRY CHEMICAL PHYSICS](#) Volume: 19 Issue: 30 Pages: 19829-19836
Published: AUG 14 2017
- 3. **Calculations of photoelectron momentum distributions and energy spectra at strong-field multiphoton ionization of sodium**
By: Bunjac, Andrej; Popovic, Duska B.; Simonovic, Nenad S. 0 0 0 0 0 0 0.00
[EUROPEAN PHYSICAL JOURNAL D](#) Volume: 71 Issue: 8 Article Number: 208
Published: AUG 2017

Select Page



Sort by: Times Cited

Date

Page of 1

3 records matched your query of the 41,289,547 in the data limits you selected.

Clarivate

Accelerating innovation

© 2018 Clarivate

[Copyright notice](#)

[Terms of use](#)

[Privacy statement](#)

[Cookie policy](#)

[Sign up for the Web of Science newsletter](#)

Follow us





На основу члана 161 Закона о општем управном поступку («Службени Лист СРЈ» број 33/97 и 31/01), и члана 120 Статута Универзитета у Београду - Физичког факултета, по захтеву АНДРЕЈА БУЊЦА, дипломираног физичара, издаје се следеће

У В Е Р Е Њ Е

АНДРЕЈ БУЊАЦ, дипломирани физичар, дана 22. јуна 2018. године, одбранио је докторску дисертацију под називом

"ИЗРАЧУНАВАЊЕ НАСЕЉЕНОСТИ АТОМСКИХ СТАЊА, УГАОНЕ РАСПОДЕЛЕ И ЕНЕРГИЈСКОГ СПЕКТРА ФОТОЕЛЕКТРОНА КОД АТОМСКИХ СИСТЕМА У ЈАКИМ ЛАСЕРСКИМ ПОЉИМА ПРИМЕНОМ ВРЕМЕНСКИ ЗАВИСНИХ МЕТОДА"

пред Комисијом Универзитета у Београду - Физичког факултета, и тиме испунио све услове за промоцију у ДОКТОРА НАУКА – ФИЗИЧКЕ НАУКЕ.

Уверење се издаје на лични захтев, а служи ради регулисања права из радног односа и важи до промоције, односно добијања докторске дипломе.

Уверење је ослобођено плаћања таксе.



ДЕКАН ФИЗИЧКОГ ФАКУЛТЕТА

Проф. др Јаблан Дојчиловић



Academy of Sciences of the Czech Republic
J. Heyrovský Institute of Physical Chemistry, v.v.i.

Dolejšková 2155/3, 182 23 Prague 8, Czech Republic

VAT Nr. CZ61388955

Phone: (+420) 28658 3014, (+420) 26605 2011

Fax: (+420) 28658 2307, e-mail: director@jh-inst.cas.cz

Dr. Andrej Bunjac
Laboratory for Atomic Collision Processes
University of Belgrade, Institute of Physics
Pregrevica 118, Belgrade 1180
Serbia

ACCEPTANCE LETTER

Dear Dr. Andrej Bunjac,

It is our pleasure to inform you that your oral contribution „Calculation of the dynamic Stark shift for sodium and the application to resonantly enhanced multiphoton ionization“ was accepted as the contributed talk (20+5 minutes) at the 7th Conference on Elementary Processes in Atomic Systems (CEPAS 2017), that will be held in September 3-6, 2017 in Průhonice, Czech Republic.

Yours sincerely,
On behalf of the local organizing committee,
Roman Čurík


In Prague 14/08/2017

.....
Dr. Roman Čurík



Cite this: *Phys. Chem. Chem. Phys.*,
2017, 19, 19829

Resonant dynamic Stark shift as a tool in strong-field quantum control: calculation and application for selective multiphoton ionization of sodium

A. Bunjac, D. B. Popović and N. S. Simonović *

A method for determining the resonant dynamic Stark shift (RDSS), based on wave-packet calculations of the populations of quantum states, is presented. It is almost insensitive to variations of the laser pulse profile, and this feature ensures generality in applications. This method is used to determine an RDSS data set for $3s \rightarrow nl$ ($n \leq 6$) transitions in sodium induced by laser pulses with peak intensities up to $7.9 \times 10^{12} \text{ W cm}^{-2}$ and wavelengths in the range from 455.6 to 1139 nm. The data are applied to analyze the photoelectron spectra (electron yield *versus* excess energy) of the sodium atom interacting with 800 nm laser radiation. Substructures observed in the experimentally measured spectra are successfully reproduced and related to the resonantly enhanced multiphoton ionization *via* specific (P and F) intermediate states.

Received 3rd April 2017,
Accepted 7th July 2017

DOI: 10.1039/c7cp02146a

rsc.li/pccp

1 Introduction

Up to the middle of the 20th century, research on the disturbance (shift and splitting) of atomic levels by an external electric field, known as the Stark effect, was limited to the case of a static electric field (the so-called dc Stark effect). The discovery and development of lasers during the 1960s stimulated the research on similar phenomena induced by alternating electromagnetic fields. The first observation of this, the so-called dynamic (or ac) Stark effect, initiated by a laser radiation field, was carried out at the end of the same decade.¹ Half a century later, a huge experience and knowledge accumulated through numerous experimental and theoretical studies gives us a detailed description of the dynamic Stark effect generated by laser radiation.

Although a number of reviews and monographs on this topic have been published,^{2–6} accurate data related to the dynamic Stark shift in a wide range of parameters are not available for most of the systems studied. This is understandable in that the dynamic Stark shift, apart from the intensity of the alternating field, depends on the frequency as well. The situation becomes more complicated when short laser pulses (ordinary or with a chirp) are used, because in that case the intensity, or both the intensity and frequency, of the radiation are fast varying parameters. The problem may be less demanding for the dynamic Stark shift which occurs under a resonance condition, the so-called resonant dynamic Stark shift (RDSS), since here the

field strength and frequency are not independent parameters. In that case, however, a perturbative treatment fails even at low intensities and, in order to obtain accurate data, more sophisticated methods must be applied.

Dynamic Stark shift, including the RDSS, today is considered as an important mechanism in the strong-field coherent (quantum) control of various atomic and molecular processes.^{7,8} The latter can be implemented through modifications of the atomic states or molecular potential surfaces such that new pathways or reaction channels, which are inaccessible in weak fields, become available.^{9,10} Determination of RDSS is, for example, essential for understanding and controlling the process of resonantly enhanced multiphoton ionization (REMPI). The dynamic shift of an atomic energy level into resonance, known as “Freeman resonance”,^{11,12} is an important phenomenon which enables strong-field coherent control over these processes. The non-static character of intermediate resonances,^{13,14} however, makes the experimental realization of REMPI more complicated. A particular challenge here is how to implement the selective ionization of an atom through a single energy level and simultaneously produce a high ion yield. By increasing the laser intensity, one increases the yield, but also spreads the electron population over multiple energy levels¹² and, in turn, reduces the selectivity.

Krug *et al.*¹⁵ recently showed, by considering the multiphoton ionization of sodium, that chirped pulses can be an efficient tool in strong-field coherent control of multiple states. In a very recent paper, Hart and coworkers¹⁶ described how improved selectivity and yield (again for sodium) can be achieved by controlling the RDSS *via* intensity (up to $10^{13} \text{ W cm}^{-2}$)

Institute of Physics, University of Belgrade, P.O. Box 57, 11001 Belgrade, Serbia.
E-mail: simonovic@ipb.ac.rs

of the laser pulse of an appropriate wavelength (800 nm). Details of the experimental equipment have been reported elsewhere.¹⁷

In this paper we present the results of the calculations of the RDSS for the sodium atom in strong laser fields performed by numerically solving the time-dependent Schrödinger equation (TDSE) within the single-electron approximation. Recently obtained experimental results^{15,16} and a lack of numerical data for sodium (beyond the perturbative approach and finite-state models) in the corresponding range of laser field parameters inspired our calculations and the analysis of the strong field quantum control of considered ionization processes.

In the next section we describe a single-electron model for alkali-metal atoms (valence electron plus atomic core), a method for numerically solving the TDSE and a way how to calculate the RDSS. In Section 3 we present the results and demonstrate how they can be used to study the REMPI. A summary and conclusions are given in Section 4.

2 Theory

2.1 The model

Singly-excited states and the single ionization of alkali-metal atoms can be described with sufficient accuracy using one-electron models. This follows from the structure of these atoms, which is that of a single valence electron moving in an orbital outside a core that consists of closed shells. In that case the valence electron is weakly bound and can be considered as moving in an effective core potential $V_{\text{core}}(r)$, which at large distances r approaches the Coulomb potential $-1/r$.

One of the simplest models for the effective core potential, applicable for alkali-metal atoms, is the Hellmann pseudopotential:¹⁸

$$V_{\text{core}}(r) = -\frac{1}{r} + \frac{A}{r} e^{-ar}. \quad (1)$$

For the sodium atom the parameters $A = 21$ and $a = 2.54920$ ¹⁹ provide the correct value of the ionization potential $I_p = 5.1391$ eV = 0.18886 a.u. (i.e. the ground state energy $E_{\text{gr}} = -I_p$) and reproduce approximately the energies of singly-excited states²⁰ (deviations are less than 1%). The applicability of pseudopotentials is based on the assumption following from the quantum defect theory²¹ that one obtains accurate approximations of the valence wave functions $\psi_{nlm}(\mathbf{r})$ outside the core if the effective potential leads to correct energies for all the states of each Rydberg series. These wave functions, both for the ground state (for sodium $\psi_{\text{gr}}(\mathbf{r}) = \psi_{300}(\mathbf{r})$) and excited states, have the standard form $\psi_{nlm}(\mathbf{r}) = R_{nl}(r)Y_{lm}(\Omega)$, where radial functions $R_{nl}(r)$ are determined numerically by solving the one-electron radial equation with pseudopotential (1).

Here we use the one-electron approach to study the single-electron excitations and the single ionization of the sodium atom in strong laser fields. Assuming that the field effects on the core electrons can be neglected (the so-called frozen-core approximation¹⁹), the Hamiltonian describing the dynamics of the valence (active) electron of the sodium (or another

alkali-metal) atom in an alternating electric field $F(t)$ reads (in atomic units)

$$H = -\frac{1}{2}\nabla^2 + V_{\text{core}}(r) - F(t)z. \quad (2)$$

We consider the linearly polarized laser pulse of the form

$$F(t) = F_{\text{peak}} \sin^2\left(\frac{\pi t}{T_p}\right) \cos\left[\omega\left(t - \frac{T_p}{2}\right) + \varphi\right], \quad (3)$$

$$0 < t < T_p$$

(otherwise $F(t) = 0$). Here ω , F_{peak} , T_p and φ are, respectively, the frequency of the laser field, the peak value of its electric component, the pulse duration and the carrier envelope phase which we set to zero. Due to the axial symmetry of the system the magnetic quantum number m of the valence electron is a good quantum number for any field strength. Since in the sodium ground state (when $F = 0$) the orbital and magnetic quantum numbers are equal to zero, in all calculations we set $m = 0$.

2.2 Energy scheme

Fig. 1 shows the excitation and ionization scheme of sodium based on energy levels corresponding to singly-excited states. Depending on the laser wavelength, different multi-photon pathways are accessible during the interaction of sodium atoms with the laser radiation. In the case of 800 nm radiation there are two dominant REMPI pathways: (i) $2 + 1 + 1$ (or $3 + 1$) ionization *via* nearly resonant two-photon transition $3s \rightarrow 4s^{22}$ and subsequent (or direct) excitation of $5p$, $6p$ and $7p$ states, giving rise to photoelectrons with s- and d-symmetry,¹⁵ and (ii) $3 + 1$ ionization *via* three-photon excitation of $4f$, $5f$ and $6f$ states,²³ giving rise to photoelectrons with d- and g-symmetry.

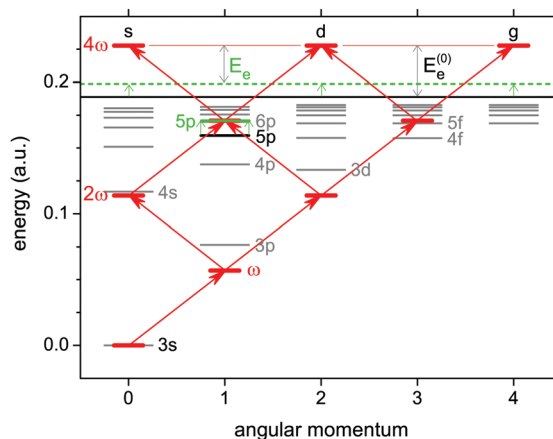


Fig. 1 Energy scheme showing the (unperturbed) lowest levels of sodium (grey lines) and possible four-photon absorption pathways from the ground state to continuum (red arrows), which arise during the interaction with 800 nm ($\omega = 0.05695$ a.u.) laser radiation. The shift of the continuum boundary (full black \rightarrow dashed green line) that corresponds to the strength of the laser field when the $5p$ level (highlighted) shifts into three-photon resonance is shown.

2.3 Numerical method

The photoexcitation and photoionization processes are simulated by calculating the evolution of the initial wave function $\psi(\mathbf{r},0) = \psi_{\text{gr}}(\mathbf{r})$, which is the lowest eigenstate of Hamiltonian (2) for $F = 0$, from $t = 0$ until a time $T_{\text{max}} > T_p$. This can be done by taking an adequate representation of the evolution operator $U(t,t + \Delta t)$ and integrating numerically the relation $\psi(\mathbf{r},t + \Delta t) = U(t,t + \Delta t)\psi(\mathbf{r},t)$ with a sufficiently small time step Δt . Here we use the second-order-difference (SOD) scheme.²⁴

$$\psi(\mathbf{r},t + \Delta t) = \psi(\mathbf{r},t - \Delta t) - 2i\Delta t H\psi(\mathbf{r},t). \quad (4)$$

Since the system described by Hamiltonian (2) is axially symmetric it is convenient to express the electron's wave function in cylindrical coordinates (ρ, φ, z) . If we write

$$\psi(\mathbf{r},t) = \Phi(\rho, z, t) \frac{e^{im\varphi}}{\sqrt{2\pi\rho}}, \quad (5)$$

where m is the magnetic quantum number, eqn (4) reduces to

$$\Phi(\rho, z, t + \Delta t) = \Phi(\rho, z, t - \Delta t) - 2i\Delta t \mathcal{H} \Phi(\rho, z, t), \quad (6)$$

where

$$\mathcal{H} = -\frac{1}{2} \left(\frac{\partial^2}{\partial \rho^2} + \frac{\partial^2}{\partial z^2} \right) + V_{\text{eff}}(\rho, z) \quad (7)$$

and

$$V_{\text{eff}} = \frac{m^2 - 1/4}{2\rho^2} + V_{\text{core}}(r) - F(t)z \quad (8)$$

with $r = (\rho^2 + z^2)^{1/2}$.

The derivatives $\partial^2 \Phi / \partial \rho^2$ and $\partial^2 \Phi / \partial z^2$ which appear in the $\mathcal{H} \Phi$ term in eqn (6) are calculated using the finite-difference method (see Appendix A). This method, however, fails at ρ values close to zero. The effective potential (8) with $m = 0$ in the limit $\rho \rightarrow 0$ behaves as $-1/8\rho^2$ where the solutions of the Schrödinger equation are $\Phi \sim \sqrt{\rho}$ and their second derivative $\partial^2 \Phi / \partial \rho^2 \sim -\rho^{-3/2} \rightarrow -\infty$. Direct application of a finite-difference formula for the determination of this derivative for small ρ then leads to a large numerical error.

The problem can be regularized by introducing the function

$$u(\rho, z) = \Phi(\rho, z) / \sqrt{\rho} \quad (9)$$

which slowly varies for ρ values close to zero. As a consequence, the ρ -derivatives of u take small (finite) values and can be determined accurately using finite-difference formulae (Appendix A). The corresponding values of $\partial^2 \Phi / \partial \rho^2$ are then obtained from the relation

$$\frac{\partial^2 \Phi}{\partial \rho^2} = -\frac{u(\rho, z)}{4\rho^{3/2}} + \frac{1}{\rho^{1/2}} \frac{\partial u}{\partial \rho} + \rho^{1/2} \frac{\partial^2 u}{\partial \rho^2}. \quad (10)$$

This approach gives the best results if we use function (9) when $\rho \leq \rho_c$, where ρ_c is a distance of the order of Bohr radius, and calculate derivatives of Φ directly for $\rho > \rho_c$.

2.4 Calculation of populations of atomic states and determination of RDSS

If the valence electron is initially in the ground state (3s), the probability of finding it in a bound state nl after the end of the laser pulse (the transition probability for this state or, equivalently, the population of the state) is

$$P_{nl} = |\langle nl | U(0, T_p) | 3s \rangle|^2 = |\langle nl | \psi(T_p) \rangle|^2. \quad (11)$$

Then the sum

$$P_{\text{ion}} = 1 - \sum_{nl} P_{nl} \quad (12)$$

determines the probability of finding the electron in a continuum (unbound) state, *i.e.* it represents the ionization probability.

The probabilities P_{nl} (populations) strongly depend on the parameters of the laser pulse (ω , T_p , F_{peak}). In particular, P_{nl} changes rapidly by varying the laser frequency ω . The maxima of functions $P_{nl}(\omega)$ occur at frequencies for which an integer (K) multiple of the photon energy ($=\omega$) coincides with the separation between the lowest (3s) and a given (nl) level of the sodium atom in the field (multi-photon resonance condition), *i.e.* when

$$K\omega = \omega_{nl,3s}, \quad (13)$$

where $\omega_{nl,3s} = E_{nl} - E_{3s}$. The additional condition (following from the selection rules for the dipole approximation) is that $K + l$ must be an even integer.

The positions of the resonant peaks in $P_{nl}(\omega)$ depend on the field strength and this dependence is a manifestation of the dynamic Stark shift. Generally, the dynamic Stark shift of atomic levels depends both on the strength and on the frequency of the field. If F is the amplitude of the alternating field, then the shift of energy level E_{nl} is

$$\delta E_{nl}(F, \omega) = E_{nl}(F, \omega) - E_{nl}^{(0)}, \quad (14)$$

where $E_{nl}^{(0)} \equiv E_{nl}(0, \omega)$ is the energy of state nl when the field is absent ($F = 0$). In the weak field limit one has $\delta E_{nl} = -\alpha_{nl}(\omega) F^2/4$, where $\alpha_{nl}(\omega)$ is known as the dynamic polarizability of the given state.² In particular, in the weak-field/high-frequency limit (*e.g.* for highly excited states nl) the polarizability $\alpha_{nl}(\omega)$ tends to the asymptotic value $-1/\omega^2$, giving $\delta E_{nl} \rightarrow F^2/4\omega^2$. This value corresponds to the vibrational energy of a free electron in the linearly polarized electromagnetic field, known as the ponderomotive potential U_p . In contrast, the shift of the ground state, for which this radiation is low-frequency, is similar to the static polarization of the atom – it is negative. Thus, the ionization potential of the atom in the laser field is higher than that of an unperturbed atom² (see Fig. 11 in the cited reference).

Since all the experiments measure not the Stark shift of a given level but the variation of the energy (frequency) of the transition from one (initial) state to another state, and since in our calculations the maxima of P_{nl} give us the separations of levels ($\omega_{nl,3s}$), we shall consider the dynamic Stark shift of the sodium atom energy levels relative to its ground state value, *i.e.*

$$\delta \omega_{nl,3s}(F, \omega) = \delta E_{nl}(F, \omega) - \delta E_{3s}(F, \omega) = \omega_{nl,3s}(F, \omega) - \omega_{nl,3s}^{(0)}, \quad (15)$$

where $\omega_{nl,3s}^{(0)} = E_{nl}^{(0)} - E_{3s}^{(0)}$.

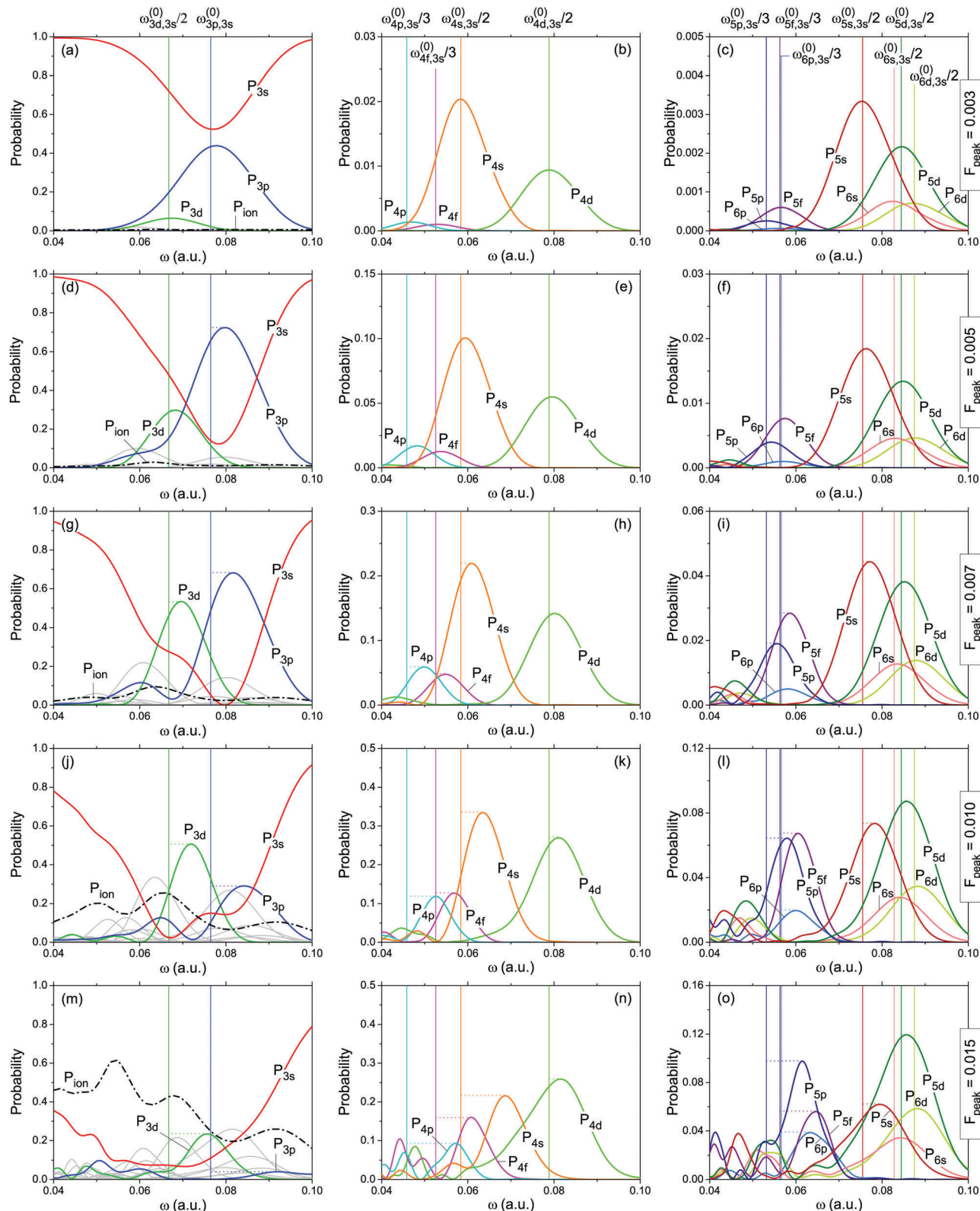


Fig. 2 Transition probabilities P_{nl} (populations) of sodium states with $n = 3, 4, 5,$ and 6 calculated for 10 fs laser pulses (3) with $F_{\text{peak}} = 0.003$ a.u. (a–c), $F_{\text{peak}} = 0.005$ a.u. (d–f), $F_{\text{peak}} = 0.007$ a.u. (g–i), $F_{\text{peak}} = 0.010$ a.u. (j–l) and $F_{\text{peak}} = 0.015$ a.u. (m–o) as functions of the laser frequency ω (full lines of different colors). Vertical lines denote the energy (frequency) of transitions from the ground state ($3s$) to other states (nl) divided by the number of absorbed photons K when $F_{\text{peak}} \rightarrow 0$. The ionization probabilities $P_{\text{ion}}(\omega)$ (dashed-dotted lines) for the five field strengths are shown in parts a, d, g, j and m.

Further, if we consider this shift strictly under the resonance condition (13), the parameters F and ω are not independent and we can write

$$\delta\omega_{nl,3s}^{\text{res}}(F) = \omega_{nl,3s}^{\text{res}}(F) - \omega_{nl,3s}^{(0)}, \quad (16)$$

where

$$\omega_{nl,3s}^{\text{res}}(F) = \omega_{nl,3s}(F, \omega_{\text{res}}) \quad (17)$$

is the separation of levels under the multiphoton resonance condition, *i.e.* at the resonant frequency

$$\omega_{\text{res}} = \omega_{nl,3s}^{\text{res}}(F)/K. \quad (18)$$

Formally, $\omega_{nl,3s}^{\text{res}}(F)$ is a solution of systems (17) and (18). However, since functions $\omega_{nl,3s}(F, \omega)$ are in principle not known, in practice we obtain $\omega_{nl,3s}^{\text{res}}(F)$ from ω_{res} values which are determined as the positions of the resonant peaks of $P_{nl}(\omega)$ at different values of F and relation (18) (which is equivalent to resonance condition (13)).

3 Results

3.1 Populations and RDSS of sodium states $n \leq 6$

In order to create an RDSS data set for sodium which might be used in the study of various strong field phenomena, we calculated the probabilities for populating the atomic levels with $n \leq 6$ under the influence of a laser pulse of the form (3) with $F_{\text{peak}} \leq 0.015$ a.u. (*i.e.* for peak intensities up to 7.90×10^{12} W cm $^{-2}$), in the range of laser frequencies ω between 0.04 and 0.1 a.u. (the corresponding wavelengths are from

1139 to 455.6 nm), and for three values of the pulse duration: $T_p = 5, 10$ and 20 fs (1 fs = 41.34 a.u.).

Fig. 2 shows the populations of the states with $n = 3$ (3s, 3p and 3d), $n = 4$ (4s, 4p, 4d and 4f), $n = 5$ (5s, 5p, 5d and 5f) and $n = 6$ (6s, 6p and 6d) calculated for the laser pulse parameters: $T_p = 10$ fs; $F_{\text{peak}} = 0.003, 0.005, 0.007, 0.010, 0.015$ a.u. and $\omega \in (0.04, 0.10)$ a.u. As explained in Section 2.4, the positions of maxima of $P_{nl}(\omega)$ can be related to resonant frequencies ω_{res} for $3s \rightarrow nl$ transitions, which determine the transition energies $\omega_{nl,3s}^{\text{res}}(F_{\text{peak}})$ at given field strengths (see eqn (18)). Once we have these energies, the RDSS values can be obtained using eqn (16).

An important feature of this method is that the peak positions of $P_{nl}(\omega)$ remain approximately the same if we vary the pulse length. For longer pulses, however, the peaks are more narrow and the resonant maxima are expected to be localized more precisely. This is demonstrated in Fig. 3 where the populations calculated for $F_{\text{peak}} = 0.007$ a.u. and three different pulse lengths ($T_p = 5, 10, 20$ fs) are compared. The above mentioned properties can be explained by the fact that the resonant frequency for a given transition essentially varies during the laser pulse due to variation of the field strength, but the ω_{res} value corresponding to a probability maximum is always related to the peak value F_{peak} .

In our calculations we favored pulses of 10 fs duration, which is for the considered problem estimated as an optimal length. Longer pulses, despite the fact that computations become more time consuming, give more complex probability distributions where the peaks related to transitions between different excited states become more pronounced. The results (energy separations $\omega_{nl,3s}^{\text{res}}(F)$) for $n \leq 6$ and six values of the

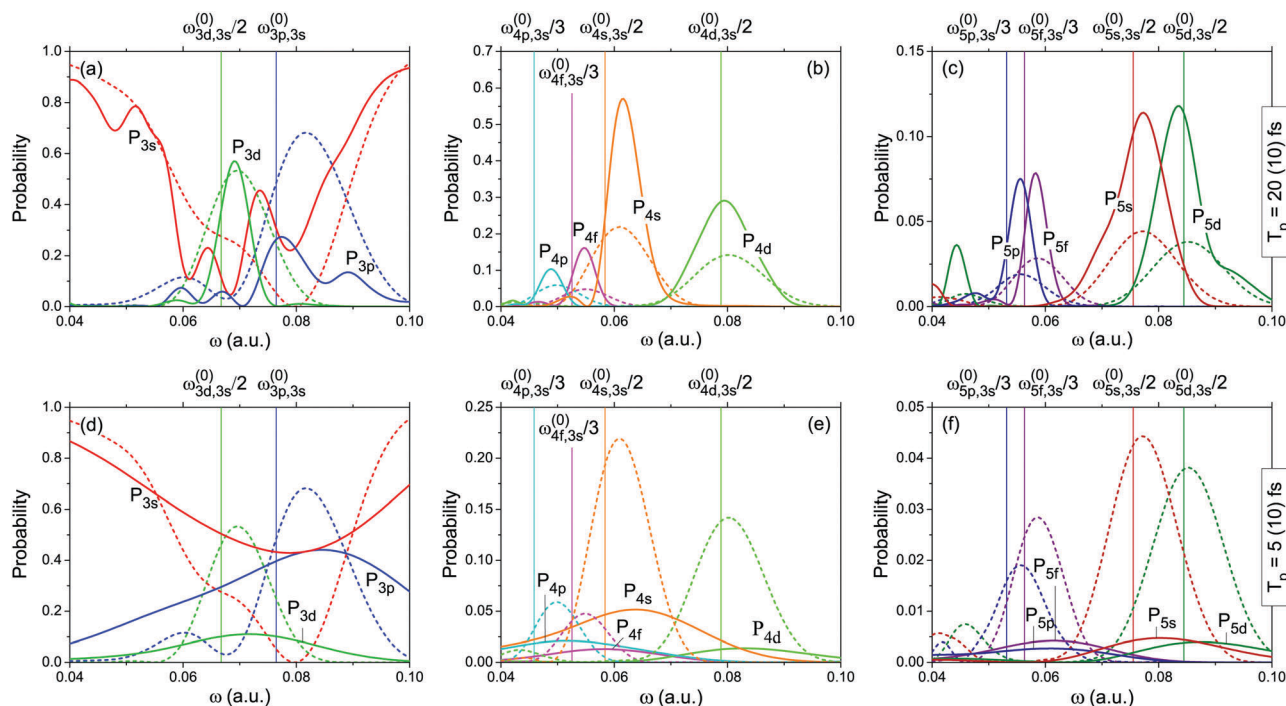


Fig. 3 Transition probabilities P_{nl} (populations) of sodium states with $n = 3, 4$, and 5 calculated for laser pulses (3) of 20 fs (a–c) and 5 fs (d–f) duration with $F_{\text{peak}} = 0.007$ a.u. as functions of the laser frequency ω (full lines of different colors). For comparison, the populations of the same states in the case of 10 fs laser pulses are shown (dotted lines).

Table 1 Energies of excited states (nl) of sodium relative to its ground state ($3s$) which are in K -photon resonance with the applied laser field of strengths $F = 0, \dots, 0.015$ a.u. These energies ($\omega_{nl,3s}^{\text{res}}(F)$) are related (by condition (18)) to the resonant laser frequencies which are obtained from the positions of maxima of the populations $P_{nl}(\omega)$. The calculations for $F > 0$ are performed using the laser pulse length $T_p = 10$ fs (see Fig. 2), except for $4f$, $5p$, $5f$ and $6p$ states where $T_p = 20$ fs. The energies for $F = 0$ are obtained by diagonalizing the one-electron Hamiltonian with pseudopotential (1) and agree well with experimental values²⁰

nl :	3p	3d	4s	4p	4d	4f	5s	5p	5d	5f	6s	6p	6d
K :	1	2	2	3	2	3	2	3	2	3	2	3	2
F (a.u.)	$\omega_{nl,3s}^{\text{res}}$ (eV)												
0	2.0800	3.6316	3.1772	3.7429	4.2912	4.2891	4.1095	4.3397	4.5966	4.5952	4.5061	4.6213	4.7620
0.003	2.1154	3.6663	3.1733	3.8297	4.2919	4.3145	4.0995	4.3813	4.6018	4.6206	4.4876	4.6532	4.7334
0.005	2.1707	3.7170	3.2346	3.9429	4.3299	4.3695	4.1535	4.4412	4.6183	4.6733	4.5219	4.7121	4.7643
0.007	2.2226	3.7889	3.3103	4.0803	4.3657	4.4540	4.1990	4.5288	4.6380	4.7545	4.5481	4.7948	4.7841
0.010	2.2912	3.9128	3.4546	4.2938	4.4123	4.6174	4.2609	4.6934	4.6643	4.9142	4.5772	4.9467	4.8053
0.015	2.5025	4.1176	3.7382	4.6655	4.4375	4.9304	4.3278	4.9962	4.6610	5.2001	4.5869	5.2287	4.8012

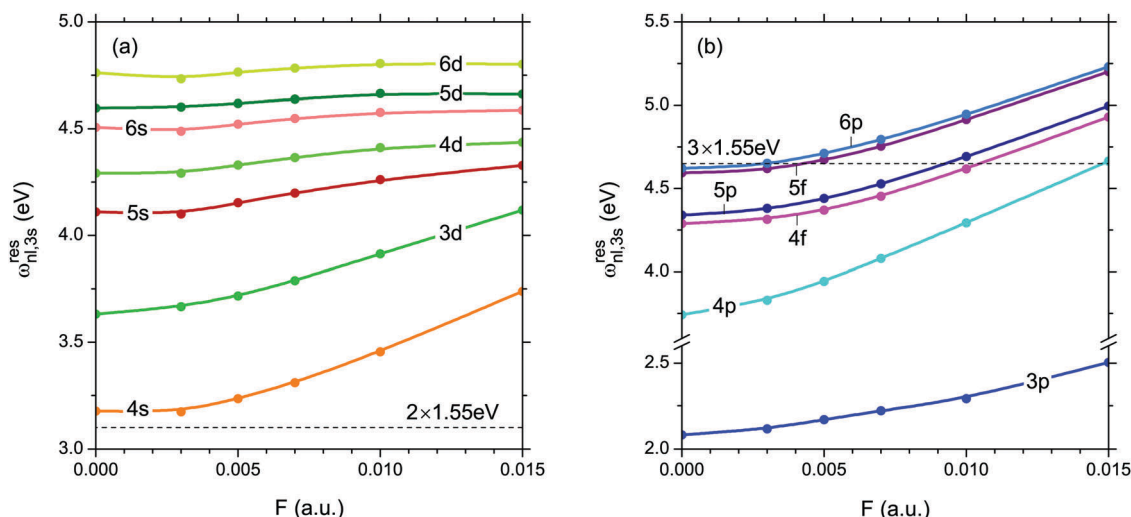


Fig. 4 The field-strength dependence of excited state energies relative to the ground state energy for the sodium atom in the laser field which is in K -photon resonance with $3s \rightarrow nl$ transitions: (a) $K = 2$, and (b) $K = 1$ (for $3s \rightarrow 3p$) and $K = 3$. Horizontal dashed lines in parts (a) and (b) mark the two- and three-photon energies, respectively, for a laser field of 800 nm wavelength.

field strength are given in Table 1 and shown (after interpolation) in Fig. 4. Although dynamic polarizabilities are in principle complex functions of the laser field parameters,^{2–6} our calculations indicate that the energy separations in the resonant case are rather smooth functions of the field strength. It is found that they increase under stronger fields, but in the perturbative regime the dynamic shift may be negative as in the static field case, particularly for the states with lower values of the polarizability (s -states, see Fig. 4a). We point out, however, that in the $F < 0.003$ a.u. range this shift is small and thus comparable to the error of locating the resonant peaks. Below we demonstrate how these results can be used to explain the structure of the photoelectron spectrum of sodium.

3.2 Analysis of the photoelectron spectrum of sodium interacting with a 800 nm laser pulse

Freeman *et al.*¹¹ have shown that when atomic states during the laser pulse transiently shift into resonance, they can be energetically resolved in the photoelectron spectrum (electron yield *versus* excess energy). Theoretically, if the multiphoton ionization occurs by absorbing N photons, the photoelectron excess energy in the weak field limit is $E_c = N\omega - I_p$. Under

stronger fields, however, the dynamic Stark shift of the ground state and that of the continuum boundary (see eqn (14) and the text below) change effectively the ionization potential I_p to $I_p - \delta E_{\text{gr}}(F, \omega) + U_p(F, \omega)$ and E_c becomes dependent on the field strength (see Fig. 1). If an intermediate state at a field strength F shifts into resonance, the photoelectron yield increases and one observes a peak at the corresponding value of E_c . Thus, the peaks in the photoelectron spectra can be related to the REMPI occurring *via* different intermediate states. If we apply the expression $\delta E_{\text{gr}} = -\alpha_{\text{gr}}(\omega)F^2/4$ and approximate the dynamic polarizability of the ground state by its static value (for sodium $\alpha_{\text{gr}}^{\text{stat}} = 162.7^{25}$), the photoelectron excess energy is determined by the formula¹⁴

$$E_c = N\omega - \left[I_p + \frac{1}{4} (\alpha_{\text{gr}}^{\text{stat}} + \omega^{-2}) F^2 \right]. \quad (19)$$

Using the data given above and eqn (19), in the following we analyze the results of recent measurements of the photoelectron yield for sodium interacting with a 800 nm laser field.¹⁶ Fig. 4(b) shows that at this wavelength (the corresponding frequency/photon energy is $\omega = 0.05695$ a.u. ≈ 1.55 eV) functions $\omega_{nl,3s}^{\text{res}}(F)$ for $4p$, $4f$, $5p$, $5f$ and $6p$ states cross the triple photon-energy ($\approx 3 \times 1.55$ eV), *i.e.* shift into resonance with the

Table 2 The values for laser field strength (electric component), laser intensity and photoelectron excess energy which characterize resonant three-photon excitation of sodium states 4p, 4f, 5p, 5f and 6p by an 800 nm laser field ($\omega \approx 1.55$ eV)

State	F (a.u.)	Intensity (W cm^{-2})	E_e (eV)
4p	0.0148	7.69×10^{12}	0.358
4f	0.0105	3.87×10^{12}	0.707
5p	0.0092	2.97×10^{12}	0.789
5f	0.0043	0.65×10^{12}	1.001
6p	0.0028	0.28×10^{12}	1.035

laser frequency, at different values of F . These field strengths, the corresponding laser intensities and the related photoelectron excess energies are given in Table 2. Comparison with the experimental results shown in Fig. 5 confirms that the most prominent peak in the photoelectron yield ($E_e \approx 0.76$ eV) is related to the REMPI *via* 4f and 5p states, whereas the local peaks at $E_e \approx 0.35$ eV and 1 eV are related to the 4p state and 5f and 6p states, respectively. (Referring to Hart *et al.*'s work¹⁶ the local peak around 1.2 eV is attributed to ionization *via* the 7p state, which is out of the set of states we considered here.) Note that for these field parameters one- or two-photon resonant transitions are not possible.

Finally, we discuss the excitation of the 4s state. One can see from Fig. 4(a) that the two-photon excitation of this state by an 800 nm laser is near resonant in the weak field limit. At higher intensities, however, detuning of the laser frequency from the resonant value increases and the transition probability for the 4s state decreases. Thus, we speculate that the 4s state does not favor significantly the excitation of P states (5p, 6p, 7p) over F states (4f, 5f, 6f), as has been expected.^{15,26} Accordingly, Fig. 2 shows that the populations of nf states are of the same order or larger than those for $(n + 1)p$ states.

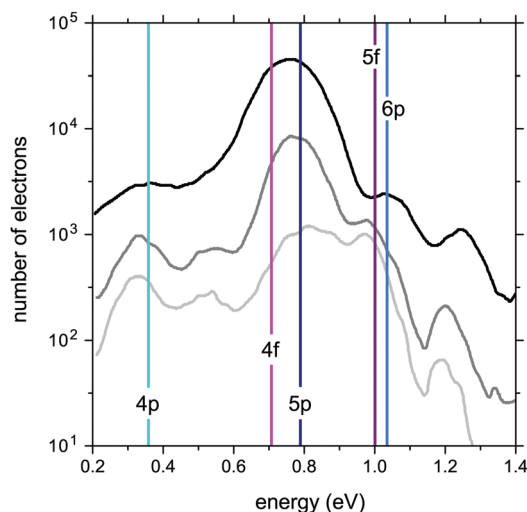


Fig. 5 Calculated values for photoelectron excess energies (vertical lines) which characterize four-photon REMPI of sodium *via* 4p, 4f, 5p, 5f and 6p states by an 800 nm laser field (from Table 2), shown together with experimentally measured electron yields *versus* photoelectron excess energies obtained for 57 fs laser pulses with peak intensities 3.5×10^{12} W cm^{-2} (white gray, lower curve), 4.9×10^{12} W cm^{-2} (gray, middle curve), and 8.8×10^{12} W cm^{-2} (black, upper curve).¹⁶

4 Summary and conclusions

We presented a method for calculating the resonant dynamic Stark shift based on a wave-packet propagation technique. We used a variant of the second-order-difference scheme that was adapted to cylindrical coordinates and applied to calculate the populations of the sodium ground and singly excited states. For this purpose, a single-electron model of the atom in a strong laser field is used. The calculations are performed for sodium levels with $n \leq 6$ and for the peak intensities of the laser pulse up to 7.90×10^{12} W cm^{-2} and wavelengths in the range from 455.6 to 1139 nm. These results are in the next step used to estimate the resonant dynamic Stark shift for $3s \rightarrow nl$ transitions. The latter results are almost insensitive to variations of the laser pulse parameters including the pulse length, envelope profile and initial phase, and this fact ensures generality in applications.

We further demonstrated how the RDSS data can be used to predict the REMPI peaks in the photoelectron spectra. We performed an analysis of the strong-field ionization of sodium interacting with an 800 nm laser pulse. The calculated positions of the peaks (photoelectron excess energies) related to the REMPI processes *via* excited P and F states (two main REMPI pathways) agree very well with recent experimental findings.¹⁶ Our calculations, however, indicate that the REMPI pathway *via* F states is not significantly suppressed, as has been expected. This conclusion is based on two findings: (i) two-photon excitation of the intermediate 4s state by an 800 nm laser at higher intensities shifts out of resonance and (ii) the populations of F states at this wavelength are of the same order or larger than those for P states. To shed light on this question, additional research, *e.g.* an accurate calculation of the photoelectron angular distribution, is recommended.

Finally, the results presented here demonstrate the ability of the proposed method to explain physical mechanisms that play an important role in the processes related to the interaction of quantum systems with strong fields and predict their behaviour under these conditions. This analysis highlights the importance of studying simpler systems for better understanding mechanisms of the strong-field coherent control of more complex systems and processes.

This work was supported by COST Action No. CM1204 (XLIC). We acknowledge support from the Ministry of Education, Science and Technological Development of Republic of Serbia under Project No. 171020.

Appendix A. Finite-difference scheme for derivatives

The first- and the second-order derivative of function $f(x)$ can be determined using finite-difference schemes:

$$\left. \frac{\partial f}{\partial x} \right|_k = \frac{1}{h} \left(\frac{1}{280} f_{k-4} - \frac{4}{105} f_{k-3} + \frac{1}{5} f_{k-2} - \frac{4}{5} f_{k-1} + \frac{4}{5} f_{k+1} - \frac{1}{5} f_{k+2} + \frac{4}{105} f_{k+3} - \frac{1}{280} f_{k+4} \right), \quad (20)$$

$$\frac{\partial^2 f}{\partial x^2} \Big|_k = \frac{1}{h^2} \left(-\frac{1}{560} f_{k-4} + \frac{8}{315} f_{k-3} - \frac{1}{5} f_{k-2} + \frac{8}{5} f_{k-1} - \frac{205}{72} f_k + \frac{8}{5} f_{k+1} - \frac{1}{5} f_{k+2} + \frac{8}{315} f_{k+3} - \frac{1}{560} f_{k+4} \right), \quad (21)$$

where x_k and $f_k = f(x_k)$ ($k = 1, \dots, N$) are the values of variables x and f on a grid with spacing h .

References

- 1 A. M. Bonch-Bruевич and V. A. Khodovoi, *Usp. Fiz. Nauk*, 1967, **93**, 71.
- 2 N. B. Delone and V. P. Krainov, *Phys.-Usp.*, 1999, **42**, 669.
- 3 M. H. Mittleman, *Introduction to the Theory of Laser-Atom Interactions*, Plenum Press, New York, 1982.
- 4 N. B. Delone and V. P. Krainov, *Atoms in Strong Light Fields*, Springer Series in Chemical Physics, Springer-Verlag, Berlin, 1985, vol. 28.
- 5 N. B. Delone and V. P. Krainov, *Multiphoton Processes in Atoms*, Springer, Heidelberg, vol. 13, 2000.
- 6 M. Fox, *Quantum Optics: An Introduction*, Oxford University Press, New York, 2006, p. 167.
- 7 H. Rabitz, R. de Vivie-Riedle, M. Motzkus and K. Kompa, *Science*, 2000, **288**, 824.
- 8 M. Shapiro and P. Brumer, *Principles of the Quantum Control of Molecular Processes*, Wiley, New York, 2003.
- 9 B. J. Sussman, D. Townsend, M. Yu. Ivanov and A. Stolow, *Science*, 2006, **314**, 278.
- 10 J. González-Vázquez, I. R. Sola, J. Santamaria and V. S. Malinovsky, *Chem. Phys. Lett.*, 2006, **431**, 231.
- 11 R. R. Freeman, P. H. Bucksbaum, H. Milchberg, S. Darack, D. Schumacher and M. E. Geusic, *Phys. Rev. Lett.*, 1987, **59**, 1092.
- 12 G. N. Gibson, R. R. Freeman and T. J. McIlrath, *Phys. Rev. Lett.*, 1992, **69**, 1904.
- 13 K. J. LaGattuta, *Phys. Rev. A: At., Mol., Opt. Phys.*, 1993, **47**, 1560.
- 14 W. Nicklich, H. Kumpfüller, H. Walther, X. Tang, H. Xu and P. Lambropoulos, *Phys. Rev. Lett.*, 1992, **69**, 3455.
- 15 M. Krug, T. Bayer, M. Wollenhaupt, C. Sarpe-Tudoran, T. Baumert, S. S. Ivanov and N. V. Vitanov, *New J. Phys.*, 2009, **11**, 105051.
- 16 N. A. Hart, J. Strohaber, A. A. Kolomenskii, G. G. Paulus, D. Bauer and H. A. Schuessler, *Phys. Rev. A*, 2016, **93**, 063426.
- 17 N. A. Hart, J. Strohaber, G. Kaya, N. Kaya, A. A. Kolomenskii and H. A. Schuessler, *Phys. Rev. A: At., Mol., Opt. Phys.*, 2014, **89**, 053414.
- 18 H. Hellmann, *J. Chem. Phys.*, 1935, **3**, 61.
- 19 M. Z. Milošević and N. S. Simonović, *Phys. Rev. A: At., Mol., Opt. Phys.*, 2015, **91**, 023424.
- 20 J. E. Sansonetti, *J. Phys. Chem. Ref. Data*, 2008, **37**, 1659.
- 21 M. J. Seaton, *Mon. Not. R. Astron. Soc.*, 1958, **118**, 504.
- 22 A. Präkelt, M. Wollenhaupt, C. Sarpe-Tudoran and T. Baumert, *Phys. Rev. A: At., Mol., Opt. Phys.*, 2004, **70**, 0634707.
- 23 A. Assion, T. Baumert, J. Helbing, V. Seyfried and G. Gerber, *Chem. Phys. Lett.*, 1996, **259**, 488.
- 24 A. Askar and A. S. Cakmak, *J. Chem. Phys.*, 1978, **68**, 2794.
- 25 J. Mitroy, M. S. Safronova and C. W. Clark, *J. Phys. B: At., Mol. Opt. Phys.*, 2010, **43**, 202001.
- 26 S. Lee, J. Lim, C. Y. Park and J. Ahn, *Opt. Express*, 2011, **19**, 2266.

Wave-packet analysis of strong-field ionization of sodium in the quasistatic regime[★]

Andrej Bunjac, Duška B. Popović, and Nenad S. Simonović^a

Institute of Physics, University of Belgrade, P.O. Box 57, 11001 Belgrade, Serbia

Received 30 December 2015

Published online 24 May 2016 – © EDP Sciences, Società Italiana di Fisica, Springer-Verlag 2016

Abstract. Strong field ionization of the sodium atom in the tunnelling and over-the-barrier regimes is studied by examining the valence electron wave-packet dynamics in the static electric field. The lowest state energy and the ionization rate determined by this method for different strengths of the applied field agree well with the results obtained using other methods. The initial period of the nonstationary decay after switching the field on is analyzed and discussed. It is demonstrated that, if the Keldysh parameter is significantly lower than one (quasistatic regime), the probability of ionization by a laser pulse can be obtained from the static rates.

1 Introduction

Interaction of atoms with strong laser fields results in a number of interesting phenomena like the above threshold ionization, high harmonic generation, atomic stabilization, non-sequential double ionization, etc. (for a review see e.g. Ref. [1] and references therein) that are unexpected from the point of view of a standard perturbative treatment. Such a treatment is in principle applicable in the case of single photon processes when the ionization rate is large even at low field intensities. It can be used partially to study multiphoton processes, but it is not applicable at sufficiently large intensities. Particularly, a more accurate approach is necessary in the case when it comes to tunnel ionization as the field becomes comparable to the atomic potential. Then the field distorts the atomic potential forming a potential barrier through which the electron can tunnel. The limiting case of this process, when the barrier is suppressed below the energy of the atomic state, is usually referred to as over-the-barrier ionization (OBI). The transition between multiphoton and tunnelling regimes is governed by the Keldysh parameter $\gamma = \omega/\omega_t$ [2], where $\omega_t^{-1} \equiv T_t = (2I_p)^{1/2}/F$ is the so-called tunnelling time and ω , F and I_p are the frequency of electromagnetic field, the peak value of electric component of the field and the ionization potential of the atom, respectively (for the sake of simplicity here and thereafter we use the atomic system of units: $e = m_e = \hbar = 4\pi\epsilon_0 = 1$). This parameter characterizes the degree of adiabaticity of the motion

through (over) the barrier: if $\gamma \gg 1$ (low-intensity/short-wavelength limit) the multiphoton ionization dominates, whereas for $\gamma \ll 1$ (high-intensity/long-wavelength limit) the tunnel ionization or OBI does. An overview of different strong-field ionization regimes can be found e.g. in reference [3].

Tunnel ionization is successfully described by the semiclassical theory due to Ammosov, Delone and Krainov (ADK) [4]. It is based on two approximations: (i) the single-electron description of tunnelling; and (ii) the quasistatic approximation. The first approximation uses the fact that most many-electron atoms can be treated as nearly hydrogenic when one of their electrons finds itself away from the core. In this single-electron picture, quantum numbers will become nonintegers. Replacing the integer quantum numbers in the rate formula for one-electron (hydrogenic) atoms [5] by these effective values one obtains the ionization rate for a given atom. The quasistatic approximation assumes that for $\gamma \ll 1$ the electric field changes slowly enough that the static tunnelling rate can be calculated for each instantaneous value of the field. Then the tunnelling rate for the alternating field can be obtained by averaging the static rates over the field period. The ADK theory accurately predicts tunnelling rates in experiments with atomic ionization in strong fields [6,7]. It also shows excellent agreement with numerical calculations in the low field limit of the tunnelling regime, i.e. for the field strengths much below the OBI domain (for hydrogen and helium see Refs. [8,9]).

Even for atoms with low ionization potentials like alkali metals, for which the tunnelling regime is reduced to a narrow interval of relatively weak fields, the ADK tunnelling rates with a correction which accounts for the Stark shift of the ground state energy agree well with numerical results obtained by the so-called complex-rotation

[★] Contribution to the Topical Issue “Advances in Positron and Electron Scattering”, edited by Paulo Lima-Vieira, Gustavo Garcia, E. Krishnakumar, James Sullivan, Hajime Tanuma and Zoran Petrovic.

^a e-mail: simonovic@ipb.ac.rs

method [10]. In the OBI domain, however, these results differ significantly and, in the absence of adequate experimental data, a check of their accuracy is welcome. In this paper we calculate the lowest state energy and ionization rate of the sodium atom in a quasistatic field as functions of the field strength by applying a wavepacket propagation technique. In addition, contrary to the complex-rotation method used in reference [10], wavepacket methods provide information about the wave function behaviour for the entire duration of the ionization process, particularly in the initial period when the decay is still nonstationary.

The paper is organized in the following way. In the next section we introduce a single electron model for the sodium atom (valence electron + atomic core) and study the strong field ionization regimes (tunnelling and OBI) in the quasistatic approximation. A time-dependent method is briefly described in Section 3. In Section 4 the results for the lowest state energies and ionization rates for sodium obtained by this method are compared with the results provided by other methods. In the same section the initial period of the nonstationary decay is analysed and discussed. Finally, it is demonstrated how the ionization probability for a given laser pulse can be obtained from the static rates.

2 The model

Chemical and optical properties of atoms depend mainly on the dynamics of the valence electrons. Particularly, in the case of alkali-metal atoms a single valence electron moves in an orbital outside a core which consists of closed shells with the total orbital momentum and spin equal to zero. Compared to the core electrons, the valence electron is weakly bound and can be considered as moving in an effective core potential (ECP) $V_{\text{core}}(r)$, which at large distances r approaches the Coulomb potential $V_C = -1/r$ (the total charge of the core for alkali is 1). The ECP is usually calibrated to produce the value $E_{\text{gr}} = -I_p$ for the ground-state energy (for sodium $I_p = 5.1391 \text{ eV} = 0.18886 \text{ a.u.}$ [11]). The energies of single-electron excitations can be represented by the Rydberg-like formula $E_{nl} = -1/2n^{*2}$, where $n^* = n - \mu_{nl}$ is the effective principal quantum number and μ_{nl} are the corresponding quantum defects. Here $n \geq n_0$, where n_0 is the lowest value of the principal quantum number n of the valence electron. The effective principal quantum number that corresponds to the ground state is therefore $n^* = (2I_p)^{-1/2}$ (for sodium $n_0 = 3$ and $n^* = 1.6271$).

One of the simplest ECP models applicable for alkali metal atoms is the Hellmann's pseudopotential [12] (see Fig. 1a)

$$V_{\text{core}}(r) = -\frac{1}{r} + \frac{A}{r} e^{-ar}. \quad (1)$$

The parameters A and a for a given atom are not uniquely determined and one can find various values proposed by different authors in reference [13,14]. For sodium, we shall use the values $A = 21$ and $a = 2.54920$ from reference [10]

with which the potential (1) reproduces exactly its ionization potential and, as close as possible, the eigenenergies of the lowest two excited states.

Using this single-electron model we study the sodium atom under the influence of a quasistatic electric field. Here we assume that the field effects to core electrons can be neglected. This so-called frozen core approximation, is good if the field is not extremely strong. Then, the dynamics of the valence electron of sodium atom in a (quasi)static electric field F is described by Hamiltonian

$$H = \frac{\mathbf{p}^2}{2} + V(\mathbf{r}), \quad (2)$$

where

$$V(\mathbf{r}) = V_{\text{core}}(r) - Fz \quad (3)$$

denotes the total potential energy. Due to the axial symmetry of the problem the z -projection of the orbital momentum l_z is an integral of motion (i.e. m is a good quantum number) and it is convenient to express all dynamical quantities in cylindrical coordinates.

The core potential and the external electric field in the total potential (3) form a potential barrier with the saddle point at the z -axis. Both the position of this point $z = z_{\text{sp}}$ (given the rule $(\partial V/\partial z)_{x=y=0} = 0$) and its height $V_{\text{sp}} = V(\mathbf{r}_{\text{sp}})$ depend on the field strength (see Figs. 1b and 1c). Since the electron can tunnel through or escape over the barrier, the atom has a nonzero probability of ionizing, even when the saddle point is well above the bound state. Thus, all states of the system described by Hamiltonian (2) have a resonant character. We shall consider here the resonance with the lowest energy. As the valence electron of an alkali-metal atom in the ground state (when $F = 0$) has its orbital and magnetic quantum numbers $l = m = 0$, the lowest resonance will be characterized by $m = 0$.

If the field is not too strong, the energy of the lowest state $E(F)$ lies below the saddle point of the barrier (see Fig. 1b) and the electron can ionize by tunnelling through the barrier. By increasing the field strength the saddle point shifts down and for strengths larger than a specific value F_s it is suppressed below the energy $E(F)$ (see Fig. 1c). Then OBI occurs. From the quantum mechanical point of view, however, there is not an essential difference between these two kinds of ionization processes.

The value of the field strength $F = F_s$ which separates the tunnelling and OBI regimes is defined by the condition $E(F) = V_{\text{sp}}(F)$. This value for sodium (but also for other alkali) is small enough that the core potentials at distances $r = |z_{\text{sp}}(F_s)|$ can be well approximated by the pure Coulomb potential [10]. Then $z_{\text{sp}} = 1/\sqrt{F}$, $V_{\text{sp}} = -2\sqrt{F}$ and the separating value F_s is the solution of equation $E(F) = -2\sqrt{F}$. By taking $E(F) \approx E(0) = -I_p$ one obtains $F_s \approx I_p^2/4 = 0.00892$.

A more accurate value for F_s can be obtained by taking into account the Stark shift of the lowest energy level. For $F \ll 1$ the Stark shift can be expanded in a Maclaurin series $\Delta E = -\alpha F^2/2! - \gamma F^4/4! - \dots$, where the first two coefficients, α and γ , are known as the dipole polarizability and the second dipole hyperpolarizability, respectively.

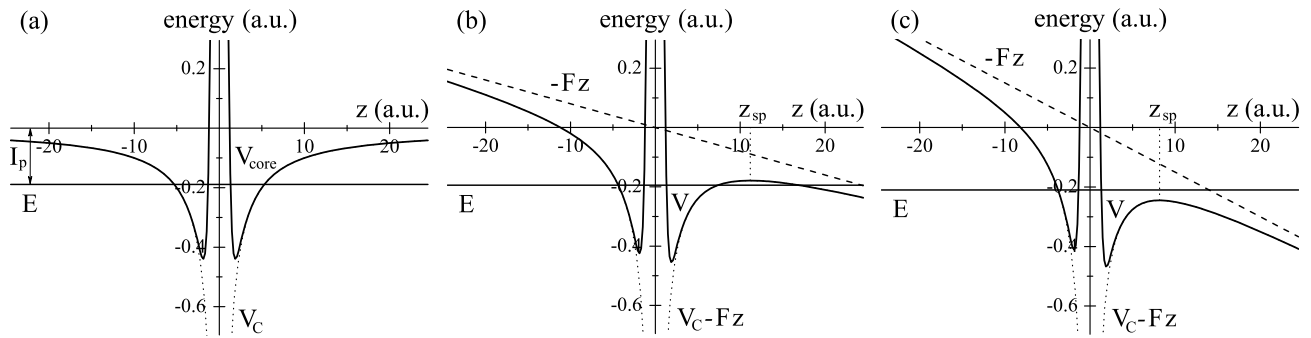


Fig. 1. Potential energy $V = V_{\text{core}}(r) - Fz$ (i.e. its $x = y = 0$ cut – full lines) and the lowest energy level E (horizontal full lines) of the valence electron of sodium atom for three different strengths of applied electric field: (a) $F = 0$, (b) $F = 0.008$ a.u. and (c) $F = 0.015$ a.u. The effective core potential $V_{\text{core}}(r)$ is represented by the Hellmann’s pseudopotential (1). The cases (b) and (c) correspond to the tunnelling and OBI regimes, respectively. For comparison, the sums (dotted lines) of the Coulomb potential $V_C = -1/r$ and the corresponding field contributions $-Fz$ (dashed lines) are shown in the same graphs.

Thus

$$E(F) = E(0) + \Delta E = -I_p - \frac{1}{2}\alpha F^2 - \frac{1}{24}\gamma F^4. \quad (4)$$

For sodium $\alpha = 162.7 \pm 0.8$ [15] and $\gamma = (9.56 \pm 0.48) \times 10^5$ [16]. The solution of equation $E(F) = -2\sqrt{F}$ with expansion (4) is $F_s = 0.00969$. The laser peak intensity that corresponds to this field strength is about 3.3×10^{12} W/cm².

Note that, since the core potential $V_{\text{core}}(r)$ approaches $V_C(r)$ in the domain $r > |z_{\text{sp}}(F_s)|$, the value F_s essentially does not depend on the ECP model. For the same reason the shape of the potential barrier and the ionization rate at weak fields (tunnelling regime) are almost independent on the form of the core potential. Thus, although there are more accurate ECP models for alkali-metal atoms, in the present analysis we are limited to the Hellmann pseudopotential as one of the simplest.

Recall that the ADK theory, which is also based on a single-electron approach, assumes the above mentioned insensitivity to the core potential. In this theory the ionization rate is given in terms of the ionization potential, quantum numbers of the atomic state and the field strength [4]. For alkali-metal atoms in the ground state the valence electron is characterized by $l = m = 0$ and the ADK formula (the variant for static fields) reduces to

$$w = |C_{n^*0}|^2 I_p \left(\frac{2F_0}{F} \right)^{2n^*-1} e^{-\frac{2F_0}{3F}}, \quad (5)$$

where $n^* = (2I_p)^{-1/2}$, $F_0 = (2I_p)^{3/2}$, and $|C_{n^*0}|^2 = 2^{2n^*} / [n^* \Gamma(n^* + 1) \Gamma(n^*)]$. Since for alkali metals the energy of the lowest state changes rapidly with F , the ADK rates can be significantly improved by applying the correction $I_p \rightarrow -E(F) = I_p - \Delta E(F)$ in (5), which accounts for the Stark shift [10].

3 The method

Resonant states can be studied efficiently using a time-dependent approach. For a known initial state wave function $\psi(\mathbf{r}, 0)$ one can obtain the wave function $\psi(\mathbf{r}, t)$

at an arbitrary time t by solving the time-dependent Schrödinger equation (TDSE). In practice this is done by taking an adequate representation of the evolution operator $U(t, t + \Delta t)$ and integrating numerically the relation $\psi(\mathbf{r}, t + \Delta t) = U(t, t + \Delta t)\psi(\mathbf{r}, t)$ with a sufficiently small time step Δt .

To study the evolution of the ground state of sodium atom after the field is switched on, we chose for the initial function $\psi(\mathbf{r}, 0)$ the lowest eigenstate of Hamiltonian (2) when $F = 0$ (i.e. the unperturbed ground state wave function of sodium within the single-electron model) and calculate its evolution at a given field strength $F > 0$ by the use of the second-order-difference (SOD) scheme [17]

$$\psi(\mathbf{r}, t + \Delta t) = \psi(\mathbf{r}, t - \Delta t) - 2i\Delta t H\psi(\mathbf{r}, t) \quad (6)$$

that is for this purpose adapted for cylindrical coordinates. Due to the axial symmetry of the system described by the Hamiltonian (2) this observable as well as the electron’s wave function do not depend on the azimuthal angle and the dynamics reduces to two degrees of freedom (ρ and z).

The energy spectrum for a given system can be obtained from the autocorrelation function

$$c(t) = \langle \psi(0) | \psi(t) \rangle \quad (7)$$

by calculating its power spectrum (i.e. $|\text{FT}[c(t)]|^2$, where $\text{FT}[c(t)]$ is the Fourier transform of $c(t)$). In this spectrum resonances appear as (approximate) Lorentzian profiles containing the information about their positions (E) and widths (Γ). If the power spectrum contains only one resonance (depending on the choice of the initial state) one has $|c(t)|^2 = e^{-wt}$, where $w = \Gamma/\hbar$ is the corresponding decay rate (hereafter we put $\hbar = 1$). Then Γ (or w) can be determined more precisely by calculating the gradient of $\ln(|c(t)|^2)$. This method will be used here to obtain the widths of the lowest state of sodium at different field strengths.

4 Results and discussion

The function $\ln(|c(t)|^2)$ for the sodium atom at different values of the applied electric field, calculated using the

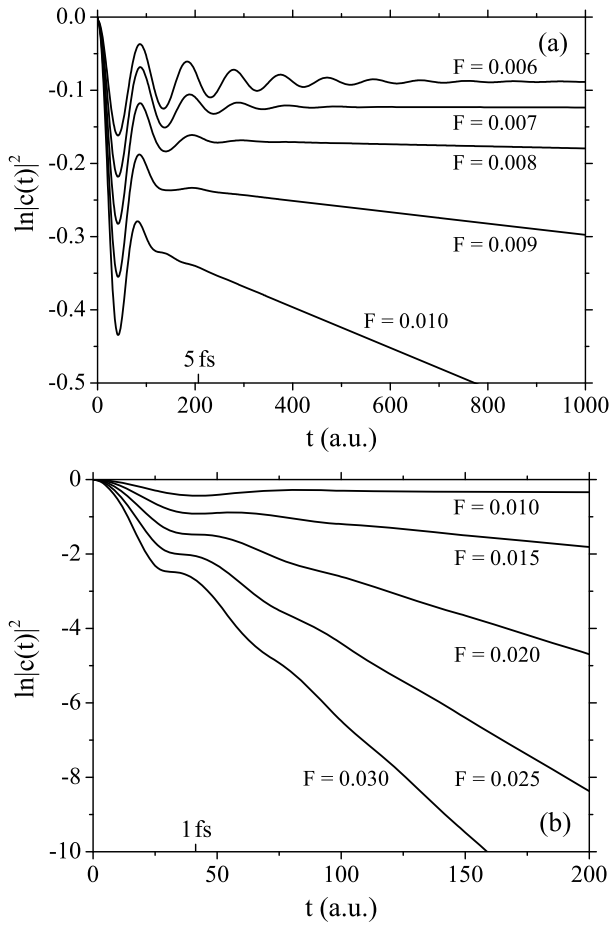


Fig. 2. Functions $\ln |c(t)|^2$ calculated for the sodium atom at different strength of the static electric field F , corresponding to: (a) the tunnelling and (b) OBI regime. The initial state $\psi(0)$ used in the autocorrelation function $c(t) = \langle \psi(0) | \psi(t) \rangle$ is the unperturbed ground state of the free atom.

model and the method described in Sections 2 and 3, respectively, is shown in Figure 2. During an initial period of the nonstationary decay the function shows damping oscillations whose relaxation time decreases by increasing the field strength. This behaviour is a consequence of the fact that the chosen initial wave function – the ground state of the unperturbed atom – is not a stationary state when the field is switched on (since in that case $V \neq V_{\text{core}}$) and behaves in the total potential as a wave packet. It can be treated as a superposition of eigenstates of Hamiltonian (2) at a given field strength F . The higher the energy of a composite eigenstate, the faster its decay through or over the potential barrier. Thus, at each reflection from the potential barrier a part of the wave packet transmits in the outer region and after some time it reduces to the lowest stationary state with a well-defined outgoing wave – the resonance wave function (see Fig. 3). This process is much faster in OBI (Fig. 2b) than in the tunnelling regime (Fig. 2a). At $F = F_s$ the duration of the nonstationary period is a few femtoseconds (1 fs = 41.34 a.u.).

Although the initial phase of the ionization process in a static field is not relevant for calculating the corre-

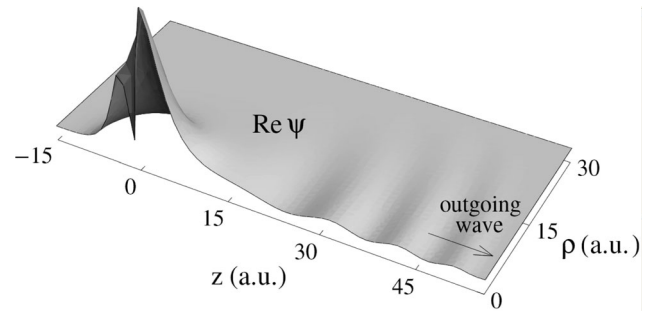


Fig. 3. The real part of the wave function $\psi(\mathbf{r})$ representing the lowest stationary state of sodium atom (the single-electron model) in the electric field of strength $F = 0.01$ a.u. This resonant state is determined by the time-propagation of the field-free sodium ground state in the total potential (3) until the state becomes stationary in the later ($t \approx 400$ a.u.).

sponding rate (we get it from $|c(t)|^2$ in the asymptotic domain), note that instant switching the field on at $t = 0$ is not a realistic situation either in the case of a static field or for laser beams. For this reason we examine the behaviour of function $|c(t)|^2$ when the field is switched on gradually. We consider the saturation function of the form $F(t) = F_{\text{stat}}[1 - \exp(-t/\tau)]$, which describes the process of establishing the electric field between two parallel conducting plates (which act as a capacitor) when connected to a dc voltage source. The time constant τ is determined by the circuit parameters. For example, if the total resistance and capacity are $R = 0.1 \Omega$ and $C = 1$ pF, respectively, then $\tau = RC = 100$ fs. The adiabaticity of switching the field in comparison with the tunnelling process can be expressed by the ratio T_t/τ (in analogy with the Keldysh parameter for ac fields). It is found that for $T_t/\tau \ll 1$ the oscillations are almost suppressed and the function $|c(t)|^2$ takes the exponentially decreasing form after the period of a few τ (see Fig. 4).

The lowest state energy and width (ionization rate) for the sodium atom in the static electric field, calculated by the wave-packet method, are shown in Table 1 for different field strengths, together with the values obtained recently by the complex-rotation method [10]. The results are in a good agreement in the field domain considered $F \in (0, 0.03)$. The numerical values from Table 1 are shown in Figure 5 together with the analytical estimations for energies and rates based on the Stark shift expansion and the ADK theory, respectively. The lowest state energy formula (4), which accounts for the Stark shift expansion up to the fourth order, agrees with numerical results approximately for $F < 1.75F_s$ (see Fig. 5a). The ionization rate obtained using the corrected ADK formula (see the last paragraph in Sect. 2) is in a very good agreement with numerical values in the tunnelling domain ($F < F_s$, see Fig. 5b).

Finally, we demonstrate that in the quasistatic regime ($\gamma \ll 1$) the ionization probability for the atom irradiated by a laser pulse can be accurately determined from the static rates. At the field strength $F = F_s$ the condition $\gamma \ll 1$ is fulfilled for sodium at wavelengths $\lambda \gg 3 \mu\text{m}$,

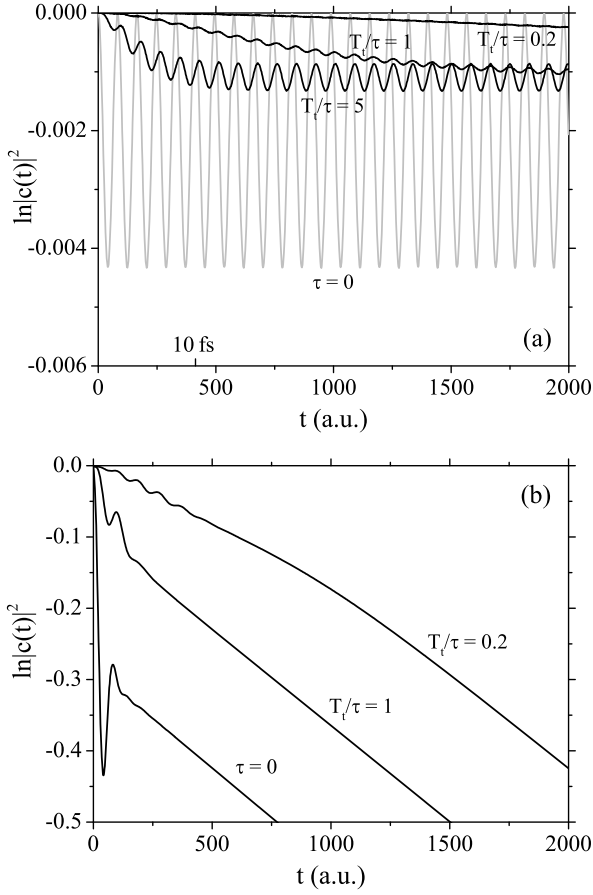


Fig. 4. Functions $\ln|c(t)|^2$ for the sodium atom in the gradually switched electric field on (see the text) of the strength: (a) $F_{\text{stat}} = 0.001$ a.u. ($=5.14$ MV/cm, $T_i = 614.6$ a.u.) and (b) $F_{\text{stat}} = 0.01$ a.u. ($=51.4$ MV/cm, $T_i = 61.46$ a.u.) for different values of the time constant τ .

whereas in the tunnelling domain λ must be even longer. We consider the linearly polarized laser pulse of the form

$$F(t) = \begin{cases} F_{\text{peak}} \sin^2(\pi t/T_p) \cos(2\pi t/T_c), & 0 < t < T_p \\ 0, & \text{otherwise} \end{cases} \quad (8)$$

and take the peak value of field strength $F_{\text{peak}} = 0.01$ a.u. (i.e. the laser peak intensity $\approx 3.5 \times 10^{12}$ W/cm²) that is close to the F_s value. We choose the optical cycle period $T_c = 1931$ a.u. (≈ 46.7 fs, $\lambda = 14$ μ m) that provides $\gamma = 0.2$ and the total pulse duration of four optical cycles ($T_p = 4T_c$). The quasistatic rate $w(F(t))$ for this pulse, obtained using the corrected ADK formula (see Eq. (5) and the text below), is shown in Figure 6a. In part (b) of the same figure the corresponding ionization probability $P_{\text{ion}}^{(\text{qs})} = \int_0^t w(F(t)) dt$ (quasistatic approximation) is compared to formula $P_{\text{ion}} = 1 - |c(t)|^2$, where $c(t)$ is the autocorrelation function obtained by solving the TDSE for the total potential (3) with the alternating field $F(t)$ of the form equation (8) (the expression for P_{ion} is the special case of general formula (see e.g. Eq. (4.28) in Ref. [18]) when the occupation probabilities for excited

Table 1. The comparison between the lowest state energies E and widths Γ of sodium obtained by the wave packet (WP) and the complex rotation (CR) method within the single-electron picture for different strengths of applied electric field F .

F	WP method		CR method	
	E	Γ	E	Γ
0.000	-0.1887	0	-0.18886	0
0.001	-0.1888	–	-0.18894	–
0.002	-0.1889	–	-0.18919	–
0.003	-0.1894	–	-0.18961	–
0.004	-0.1900	–	-0.19020	–
0.005	-0.1908	–	-0.19096	–
0.006	-0.1916	6×10^{-8}	-0.19190	–
0.007	-0.1928	1.32×10^{-6}	-0.19303	1.276×10^{-6}
0.008	-0.1941	1.42×10^{-5}	-0.19437	1.279×10^{-5}
0.009	-0.1957	7.59×10^{-5}	-0.19595	7.426×10^{-5}
0.010	-0.1976	2.78×10^{-4}	-0.19778	2.684×10^{-4}
0.011	-0.1998	7.28×10^{-4}	-0.19986	7.097×10^{-4}
0.012	-0.2021	1.53×10^{-3}	-0.20215	1.503×10^{-3}
0.013	-0.2046	2.74×10^{-3}	-0.20461	2.691×10^{-3}
0.014	-0.2071	4.36×10^{-3}	-0.20717	4.287×10^{-3}
0.015	-0.2097	6.37×10^{-3}	-0.20979	6.261×10^{-3}
0.016	-0.2123	8.69×10^{-3}	-0.21245	8.577×10^{-3}
0.017	-0.2150	0.0113	-0.21513	0.01120
0.018	-0.2176	0.0142	-0.21780	0.01409
0.019	-0.2201	0.0174	-0.22047	0.01721
0.020	-0.2227	0.0208	-0.22312	0.02051
0.021	-0.2252	0.0243	-0.22575	0.02400
0.022	-0.2278	0.0280	-0.22836	0.02763
0.023	-0.2302	0.0317	-0.23094	0.03139
0.024	-0.2327	0.0356	-0.23351	0.03527
0.025	-0.2351	0.0395	-0.23605	0.03928
0.026	-0.2376	0.0434	-0.23856	0.04331
0.027	-0.2399	0.0475	-0.24106	0.04745
0.028	-0.2423	0.0517	-0.24353	0.05166
0.029	-0.2446	0.0561	-0.24598	0.05595
0.030	-0.2469	0.0608	-0.24841	0.06025

atomic states are almost zero, which is the case in this example). Functions $P_{\text{ion}}^{(\text{qs})}(t)$ and $P_{\text{ion}}(t)$ are significantly different during the laser pulse because the former represents the probability of transition from the initial atomic state to the asymptotic continuum state (outgoing wave), whereas the latter is the probability of transition from the initial state to any unbound state, including those when the electron is temporary ejected and recaptured in the next half-cycle of the field. These two functions, however, approach each other whenever the field becomes zero and this fact allows us to determine the total ionization probability (when the pulse is over) from the static rates. The difference between $P_{\text{ion}}(T_p)$ and $P_{\text{ion}}^{(\text{qs})}(T_p)$ in this example

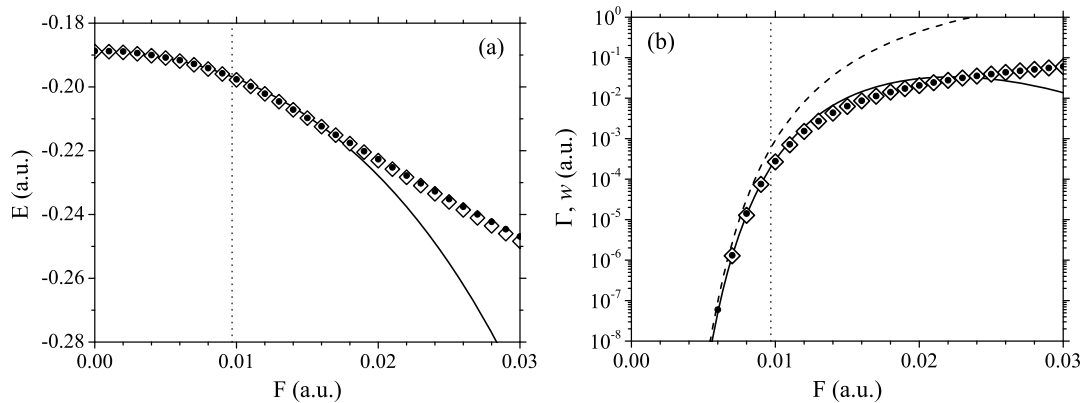


Fig. 5. The energies (a) and widths (b) of the lowest state of the sodium atom at different strengths of applied electric field. The results obtained by the wave-packet propagation method (present work) are marked by full circles. For comparison, the corresponding results obtained by the complex-rotation method [10] are shown (open ‘diamonds’). In addition, the lowest state energy as a function of the field strength determined by the 4th order expansion formula (4) (full line) is shown in part (a), and the ionization rates determined by the original ADK formula (5) (dashed line) as well as by the ADK formula with the Stark shift correction (4) (full line) are shown in part (b). Vertical dotted lines mark the field strengths F_s dividing the tunnelling and OBI areas.

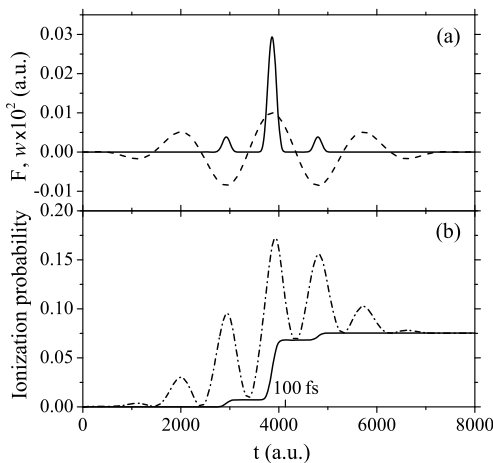


Fig. 6. (a) The laser pulse of the form (8) with $F_{\text{peak}} = 0.01$ a.u., $T_c = 1931$ a.u., $T_p = 4T_c$ (dashed line) and the corresponding quasistatic ionization rate $w(F(t))$ for sodium (full line). (b) The ionization probability determined by integrating the quasistatic rate (full line) and by solving the TDSE with the alternating field (8) exactly (dash-dot line).

($\gamma = 0.2$) is less than one percent, but it increases significantly for larger values of the Keldysh parameter.

We dedicate this paper to the occasion of Professor Michael Allan’s retirement, in recognition of his scientific contributions to the field of electron scattering. One of us (DBP) would also like to express her deep gratitude to Professor Michael Allan, her post-doc research supervisor, for his patient guidance, enthusiastic encouragement and useful critiques during her years working with him. This work was supported by the COST Action No. CM1204 (XLIC). We acknowledge support from the Ministry of Education, Science and Technological Development of Republic of Serbia under Project No. 171020.

References

1. P. Agostini, L.F. DiMauro, *Adv. At. Mol. Opt. Phys.* **61**, 117 (2012)
2. L.V. Keldysh, *Sov. Phys. J. Exp. Theor. Phys.* **20**, 1307 (1965)
3. M. Protopapas, C.H. Keitel, P.L. Knight, *Rep. Prog. Phys.* **60**, 389 (1997)
4. M.V. Ammosov, N.B. Delone, V.P. Krainov, *Sov. Phys. J. Exp. Theor. Phys.* **64**, 1191 (1986)
5. L.D. Landau, E.M. Lifshitz, *Quantum Mechanics* (Pergamon Press, Oxford, 1991), p. 296
6. S. Augst, D.D. Meyerhofer, D. Strickland, S.L. Chin, *J. Opt. Soc. Am. B* **8**, 858 (1991)
7. W. Xiong, S.L. Chin, *Sov. Phys. J. Exp. Theor. Phys.* **72**, 268 (1991)
8. A. Scrinzi, M. Geissler, T. Brabec, *Phys. Rev. Lett.* **83**, 706 (1999)
9. J.S. Parker, G.S.J. Armstrong, M. Boca, K.T. Taylor, *J. Phys. B* **42**, 134011 (2009)
10. M.Z. Milošević, N.S. Simonović, *Phys. Rev. A* **91**, 023424 (2015)
11. J.E. Sansonetti, W.C. Martin, *J. Phys. Chem. Ref. Data* **34**, 1559 (2005)
12. H. Hellmann, *J. Chem. Phys.* **3**, 61 (1935)
13. G.A. Hart, P.L. Goodfriend, *J. Chem. Phys.* **53**, 448 (1970)
14. W.H.E. Schwarz, *J. Chem. Phys.* **54**, 1842 (1971)
15. J. Mitroy, M.S. Safronova, C.W. Clark, *J. Phys. B* **43**, 202001 (2010)
16. A.J. Thakkar, C. Lupinetti, *Atomic Polarizabilities and Hyperpolarizabilities: A Critical Compilation*, in *Atoms, Molecules, and Clusters in Electric Fields: Theoretical Approaches to the Calculation of Electric Polarizability*, edited by George Maroulis (Imperial College Press, 2006), p. 505
17. A. Askar, A.S. Cakmak, *J. Chem. Phys.* **68**, 2794 (1978)
18. F. Grossmann, *Theoretical Femtosecond Physics* (Springer-Verlag, Berlin, 2008)

Calculations of photoelectron momentum distributions and energy spectra at strong-field multiphoton ionization of sodium^{*}

Andrej Bunjac, Duška B. Popović, and Nenad S. Simonović^a

Institute of Physics, University of Belgrade, P.O. Box 57, 11001 Belgrade, Serbia

Received 21 April 2017 / Received in final form 27 May 2017

Published online 8 August 2017 – © EDP Sciences, Società Italiana di Fisica, Springer-Verlag 2017

Abstract. Multiphoton ionization of sodium by a femtosecond laser pulse of 760 nm wavelength and different peak intensities is studied by inspecting the photoelectron angular and momentum distributions and the energy spectra. For this purpose a single-electron model of the atom interacting with the electromagnetic field is used, and the distributions are determined by calculating the evolution of the electron wave function. Beside the most prominent distribution maxima related to the four-photon ionization, the five-photon (above-threshold) ionization peaks are observed. Substructures in the main (nonresonant) maximum in the photoelectron spectra at the four-photon ionization are related to the resonantly enhanced multiphoton ionization via intermediate $4s$, $4f$, $5p$, $5f$ and $6p$ states.

1 Introduction

Interaction of strong laser fields with atoms may lead to their photoionization even when the single photon energy is lower than the ionization potential of atom. In that case the atom absorbs several photons simultaneously and this process is known as the multiphoton ionization (MPI, see e.g. Refs. [1–4]). Contrary to the single photon ionization, where the ionization rate is large even at very low intensities, the probability for multiphoton processes is much lower and they occur only at sufficiently strong fields. For this reason a perturbative treatment, which is a valid approach in describing the single photon ionization, in the case of MPI usually fails.

A clear indication of the non-perturbative regime in the interaction of an atom with the radiation is the so-called above threshold ionization (ATI), in which the atom absorbs more photons than the minimum required [5] (see also Refs. [1–4]). Another phenomenon of a particular interest is the resonantly enhanced multiphoton ionization (REMPI) [6] (see also Refs. [1–4]). It takes place if the MPI process occurs via an intermediate state whose excitation energy coincides with an integer multiple of the photon energy. Although these phenomena can be recognized in the photoelectron energy spectrum, for their deeper analysis it is recommended to calculate the photoelectron angular and momentum distributions (PAD and PMD) containing the information about multiphoton absorption pathways.

Here we study the MPI of the sodium atom induced by a short (10 fs) laser pulse of 760 nm wavelength. Using the single-electron model we calculate the PAD and PMD by solving numerically the time-dependent Schrödinger equation. At the considered wavelength at least four photons must be absorbed to ionize the atom and, depending on the laser intensity, the REMPI via several intermediate states may occur. A similar theoretical analysis, together with experimental results, has been reported earlier for lithium [7]. Recent measurements on sodium [8,9] revealed REMPI structures in its photoelectron spectra, stimulating the analysis presented in this paper.

In the next section we describe the model and in Section 3 consider the excitation and ionization schemes. A method for calculating the photoelectron angular and momentum distributions is briefly described in Section 4. In Section 5 we present the calculated distributions and analyze the photoelectron energy spectra. A summary is given in Section 6.

2 The model

Singly-excited states and the single ionization of the alkali-metal atoms are, for most purposes, described in a satisfactory manner using one-electron models. This follows from the structure of these atoms, which is that of a single valence electron moving in an orbital outside a core consisting of closed shells. In that case the valence electron is weakly bound and can be considered as moving in an effective core potential $V_{\text{core}}(r)$, which at large distances r approaches the Coulomb potential $-1/r$. One of the simplest models for the effective core potential, applicable

^{*} Contribution to the Topical Issue “Physics of Ionized Gases (SPIG 2016)”, edited by Goran Popovic, Bratislav Obradovic, Dragana Maric and Aleksandar Milosavljevic.

^a e-mail: simonovic@ipb.ac.rs

for the alkali-metal atoms, is the Hellmann pseudopotential [10] (in atomic units)

$$V_{\text{core}}(r) = -\frac{1}{r} + \frac{A}{r} e^{-ar}. \quad (1)$$

In the case of sodium the parameters $A = 21$ and $a = 2.54920$ [11] provide the correct value for the ionization potential $I_p = 5.1391 \text{ eV} = 0.18886 \text{ a.u.}$ and reproduce approximately the energies of singly-excited states [12] (deviations are less than 1%). The associated eigenfunctions are one-electron approximations of these states and have the form $\psi_{nlm}(\mathbf{r}) = R_{nl}(r)Y_{lm}(\Omega)$. Radial functions $R_{nl}(r)$ can be determined numerically by solving the corresponding radial equation.

Here we use the one-electron approach to study the single-electron excitations and the single ionization of the sodium atom in a strong laser field. Assuming that the field effects on the core electrons can be neglected (the so-called frozen-core approximation [11]), the Hamiltonian describing the dynamics of valence (active) electron of the sodium atom in an alternating electric field $F(t)$ reads (in atomic units)

$$H = -\frac{1}{2}\nabla^2 + V_{\text{core}}(r) - F(t)z. \quad (2)$$

We consider the linearly polarized laser pulse of the form

$$F(t) = F_{\text{peak}} \sin^2(\pi t/T_p) \cos \omega t, \quad 0 < t < T_p \quad (3)$$

(otherwise $F(t) = 0$). Here ω , F_{peak} and T_p are the frequency of the laser field, the peak value of its electric component and the pulse duration, respectively. Due to axial symmetry of the system the magnetic quantum number m of the valence electron is a good quantum number for any field strength. Since in the sodium ground state (when $F = 0$) the orbital and magnetic quantum numbers are equal to zero, in our calculations we set $m = 0$.

3 Excitation scheme and photoelectron excess energy

Figure 1 shows the lowest energy levels corresponding to singly-excited states of sodium and possible multiphoton absorption pathways during the interaction of the atom with a 760 nm laser radiation ($\omega = 0.06 \text{ a.u.}$). Generally, if the MPI occurs by absorbing N photons, the photoelectron excess energy in the weak field limit is

$$E_e^{(0)} = N\omega - I_p. \quad (4)$$

In a strong field case, however, the dynamic Stark shift of the ground state δE_{gr} , as well as that of the continuum boundary δE_{cont} , change effectively the ionization potential I_p to $I_p - \delta E_{\text{gr}}(F, \omega) + \delta E_{\text{cont}}(F, \omega)$ and E_e becomes dependent on the field strength. Using expression $\delta E_{\text{gr}} = -\alpha_{\text{gr}}(\omega)F^2/4$ for the ground state shift [13], in which the dynamic polarizability is approximated by its

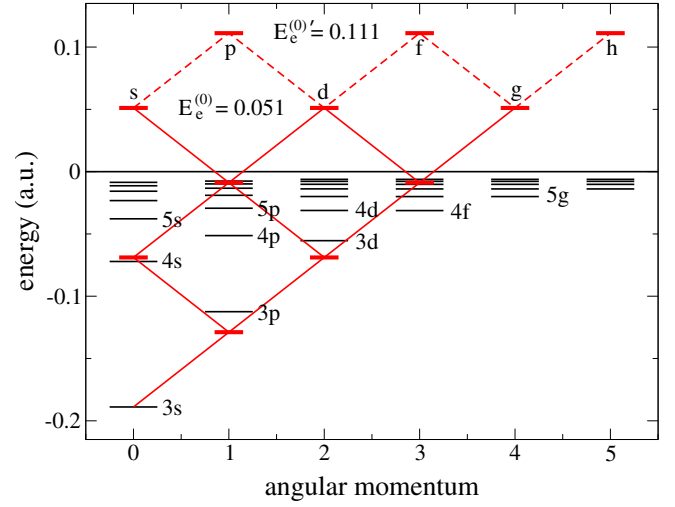


Fig. 1. Energy scheme of sodium showing the lowest singly excited states [12] and possible four-photon and five-photon (ATI) absorption pathways ($\omega = 0.06 \text{ a.u.}$) from the $3s$ ground state to the continuum.

static value (for sodium $\alpha_{\text{gr}}^{\text{stat}} = 162.7 \text{ a.u.}$ [14]), and relation $\delta E_{\text{cont}} \approx U_p$ for the continuum boundary shift [13], where $U_p = F^2/4\omega^2$ is the ponderomotive potential of electromagnetic field, the photoelectron excess energy is approximately given by formula

$$E_e = N\omega - [I_p + \frac{1}{4}(\alpha_{\text{gr}}^{\text{stat}} + \omega^{-2})F^2]. \quad (5)$$

The energy level diagram in Figure 1 illustrates that from the ground state ($3s$) at least four photons with $\omega = 0.06 \text{ a.u.}$ are required to reach the continuum. In the low-intensity regime, this nonresonant MPI is a dominating process and $E_e \approx E_e^{(0)} = 0.051 \text{ a.u.} = 1.39 \text{ eV}$. If five photons are absorbed, the photoelectron excess energy will be $E_e^{(0)'} = E_e^{(0)} + \omega = 0.111 \text{ a.u.} = 3.02 \text{ eV}$ (the first ATI peak). By increasing the field strength the excess energy E_e decreases, but on the other hand the REMPI via different intermediate states take place. The latter can be recognized as a substructure in the main (nonresonant) peak in the photoelectron spectrum. This spectrum can be obtained from the PMD, whose calculation is described in the next section.

4 Numerical method

The photoionization process is simulated by calculating the evolution of the initial wave function $\psi(\mathbf{r}, 0)$, which is the lowest eigenstate of Hamiltonian (2) at $t = 0$ (and $F = 0$), until a time $t > T_p$. This can be done by taking an adequate representation of the evolution operator $U(t, t + \Delta t)$ and integrating numerically the relation $\psi(\mathbf{r}, t + \Delta t) = U(t, t + \Delta t)\psi(\mathbf{r}, t)$ with a sufficiently small time step Δt . Here we use the second-order-difference (SOD) scheme [15]

$$\psi(\mathbf{r}, t + \Delta t) = \psi(\mathbf{r}, t - \Delta t) - 2i\Delta t H\psi(\mathbf{r}, t). \quad (6)$$

Since the system described by Hamiltonian (2) is axially symmetric, it is convenient to express the electron's wave function in cylindrical coordinates (ρ, φ, z) . If we write

$$\psi(\mathbf{r}, t) = \Phi(\rho, z, t) \frac{e^{im\varphi}}{\sqrt{2\pi\rho}}, \quad (7)$$

equation (6) reduces to

$$\Phi(\rho, z, t + \Delta t) = \Phi(\rho, z, t - \Delta t) - 2i\Delta t \mathcal{H}\Phi(\rho, z, t), \quad (8)$$

where

$$\mathcal{H} = -\frac{1}{2} \left(\frac{\partial^2}{\partial \rho^2} + \frac{\partial^2}{\partial z^2} \right) + V_{\text{eff}}(\rho, z) \quad (9)$$

and

$$V_{\text{eff}} = \frac{m^2 - 1/4}{2\rho^2} + V_{\text{core}}(r) - F(t)z \quad (10)$$

with $r = (\rho^2 + z^2)^{1/2}$.

The second order derivatives of Φ (appearing in term $\mathcal{H}\Phi$ in Eq. (8)) are calculated using the finite-difference scheme

$$\begin{aligned} \left. \frac{\partial^2 f}{\partial x^2} \right|_k &= \frac{1}{h^2} \left(-\frac{1}{560} f_{k-4} + \frac{8}{315} f_{k-3} - \frac{1}{5} f_{k-2} \right. \\ &\quad + \frac{8}{5} f_{k-1} - \frac{205}{72} f_k + \frac{8}{5} f_{k+1} \\ &\quad \left. - \frac{1}{5} f_{k+2} + \frac{8}{315} f_{k+3} - \frac{1}{560} f_{k+4} \right), \quad (11) \end{aligned}$$

where x_k and $f_k = f(x_k)$ ($k = 1, \dots, N$) are the values of variables x and f on a grid with spacing h . This method, however, fails at $\rho \rightarrow 0$ because there effective potential (10) with $m = 0$ behaves as $-1/8\rho^2$, where the solutions of the Schrödinger equation are $\Phi \sim \sqrt{\rho}$ and $\partial^2 \Phi / \partial \rho^2 \sim -\rho^{-3/2} \rightarrow -\infty$.

The problem can be regularized by introducing the function

$$u(\rho, z) = \Phi(\rho, z) / \sqrt{\rho} \quad (12)$$

which is slowly varying for values of ρ close to zero and the ρ -derivatives of u can be calculated with a sufficient accuracy. The corresponding values of $\partial^2 \Phi / \partial \rho^2$ are then obtained from the relation

$$\frac{\partial^2 \Phi}{\partial \rho^2} = -\frac{u(\rho, z)}{4\rho^{3/2}} + \frac{1}{\rho^{1/2}} \frac{\partial u}{\partial \rho} + \rho^{1/2} \frac{\partial^2 u}{\partial \rho^2}. \quad (13)$$

The first-order derivatives are calculated using the scheme

$$\begin{aligned} \left. \frac{\partial f}{\partial x} \right|_k &= \frac{1}{h} \left(\frac{1}{280} f_{k-4} - \frac{4}{105} f_{k-3} + \frac{1}{5} f_{k-2} - \frac{4}{5} f_{k-1} \right. \\ &\quad \left. + \frac{4}{5} f_{k+1} - \frac{1}{5} f_{k+2} + \frac{4}{105} f_{k+3} - \frac{1}{280} f_{k+4} \right). \quad (14) \end{aligned}$$

The presented approach gives the best results if we use function (12) when $\rho \leq \rho_c$, where ρ_c is a distance of the order of Bohr radius, and calculate derivatives of Φ

directly for $\rho > \rho_c$. In our calculation the wave functions are represented by $N_\rho \times N_z = 1024 \times 2048$ discrete values on the grid covering the area $0 < \rho < 500$ a.u., -500 a.u. $< z < 500$ a.u. In order to suppress the edge effects such as reflection, an absorbing potential have been added at outer part of the area.

The momentum distribution of photoelectrons is determined from the electron probability density in the momentum space $|\bar{\psi}(\mathbf{k}, t)|^2$ at $t > T_p$. In order to make this distribution well visible, it is important to separate the outgoing wave $\psi_{\text{out}}(\mathbf{r}, t)$ from the inner (bound) part of the wave function. This can be done by propagating the wave function until the time when the overlap between these two parts becomes insignificant. The transformation of the outgoing wave from the coordinate to momentum representation is done by the Fourier transform. In our case, due to axial symmetry of the problem, it is not necessary to calculate the full 3D Fourier transform. The momentum distribution in the (k_ρ, k_z) -subspace can be obtained directly from the function $\psi_{\text{out}}(\rho, z)$ by the transformation

$$\bar{\psi}(k_\rho, k_z) = \frac{1}{(2\pi)^2} \int_{-\infty}^{\infty} dz e^{-ik_z z} \int_0^{\infty} \rho d\rho J_0(k_\rho \rho) \psi(\rho, z), \quad (15)$$

where J_0 is the Bessel function of the first kind of order zero. The integral in terms of z -coordinate, which appears in this expression, can be evaluated by applying the FFT algorithm.

The photoelectron energy spectrum can be obtained by averaging the probability distribution $|\bar{\psi}(k_\rho, k_z, t)|^2$ at a time $t \gg T_p$ along semicircles $k_\rho^2 + k_z^2 = 2E_e$ corresponding to different photoelectron excess energies E_e .

5 Results

5.1 Angular and momentum distributions

We consider the photoionization of the sodium atom by 760 nm ($\omega = 0.06$ a.u.) laser pulse of the form (3) and 10 fs duration ($T_p = 413.4$ a.u.) for three values of the field strength: $F = 0.007, 0.01$ and 0.015 a.u. (the corresponding laser peak intensities are: 1.72, 3.51 and 7.90 TW/cm²).

Figure 2 shows the probability distribution $|\psi(\mathbf{r}, t)|^2$ of the active (valence) electron at $t = 1000$ a.u. and $t = 1200$ a.u. for the strength $F = 0.007$ a.u. The outgoing wave determines the PAD. Apart from the strong emission along the laser polarization direction ($\vartheta = 0^\circ$ and 180°) the distribution also shows maxima at $\vartheta \approx 45^\circ$, $\vartheta = 90^\circ$ and $\vartheta \approx 135^\circ$. The observed PAD relates to a superposition of the accessible emitted partial waves. In the case of four-photon absorption s, d and g partial waves can be emitted (see Fig. 1). The nodal structure of the outgoing wave in Figure 2 indicates that in this case the g partial wave is dominant (four-minima/five-maxima), i.e. the main pathway goes via F -states. This conclusion is in agreement with the nodal structure of the inner (bound) part of wave function (having four maxima), indicating

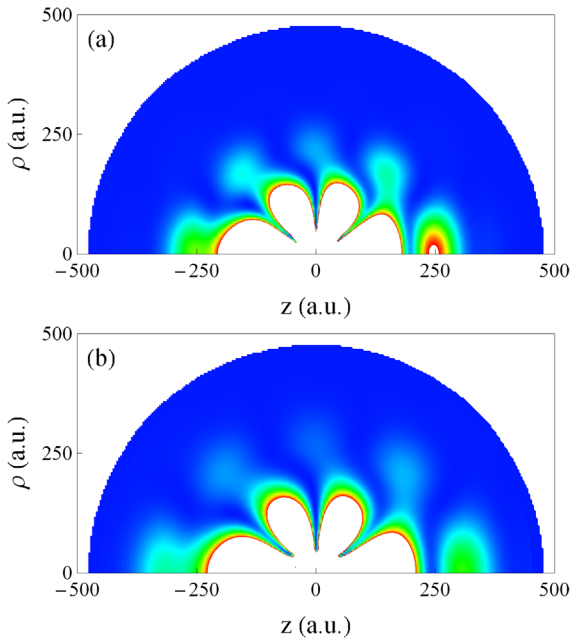


Fig. 2. Probability distribution $|\psi(\mathbf{r}, t)|^2$ of the active electron of sodium atom irradiated by the 10 fs duration laser pulse of the form (3) with $\omega = 0.06$ a.u. and $F = 0.007$ a.u. at: (a) $t = 1000$ a.u. and (b) $t = 1200$ a.u. The outgoing wave (with five maxima) determines the photoelectron angular distribution.

that, when the pulse is over, ionized atoms are in a coherent state with a significant contribution of F -states.

The PMD shows a similar structure as the PAD, but the maxima are located at semicircles of radius $k_e \approx k_e^{(0)} \equiv (2E_e^{(0)})^{1/2} = 0.32$ a.u. Shortly after the ionization, when photoelectrons did not yet reach the asymptotic area, their momenta are larger than $k_e^{(0)}$ (see Fig. 3a), but later they approach the asymptotic value (Fig. 3b). The remaining difference ($k_e - k_e^{(0)} \approx -0.02$ a.u.) can be attributed to the dynamic Stark shift.

Besides the MPI with four photons, in Figure 3 the ATI structure related to the five-photon absorption can be observed. In the later case, according to the energy level diagram in Figure 1, the photoelectron momentum in the weak field limit is $k_e^{(0)'} \equiv (2E_e^{(0)'})^{1/2} = 0.47$ a.u. and p , f and h partial waves can be emitted. The ATI structure in Figure 3 is indeed located near $k_e^{(0)'}$ and contains five minima which is a feature of h waves. It is noticed that ATI peaks are more prominent shortly after the end of the pulse (compare Figs. 2a and 2b). This feature may be explained by the fact that the electrons which absorb more photons than required have larger momenta ($k_e' > k_e$) and, thus, escape faster.

5.2 Resonantly enhanced multiphoton ionization of sodium

Freeman et al. [6] have shown that when atomic states during the laser pulse transiently shift into resonance, they can be energetically resolved in the photoelectron spec-

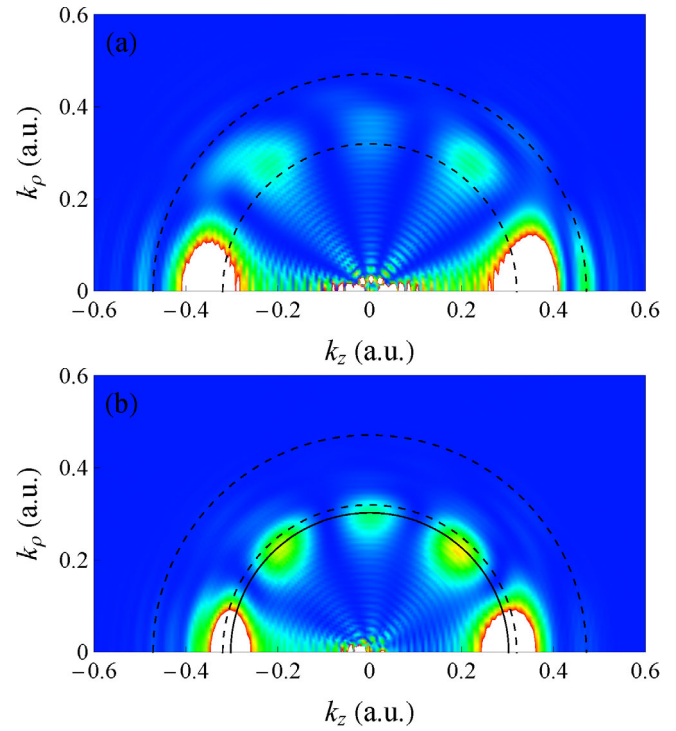


Fig. 3. The photoelectron momentum distribution for the process shown in Figure 2 at: (a) $t = 800$ a.u. and (b) $t = 1000$ a.u. Dashed semicircles denote the expected values of the momentum for the four-photon (MPI) and five-photon (ATI) processes in the weak field limit ($k_e^{(0)} \equiv (2E_e^{(0)})^{1/2} = 0.32$ a.u. and $k_e^{(0)'} \equiv (2E_e^{(0)'})^{1/2} = 0.47$ a.u.). The full semicircle corresponds to the photoelectron momentum at the four-photon ionization when the dynamic Stark shifts of the ground state and the ionization boundary (see Eq. (5)) are taken into account ($k_e \equiv (2E_e)^{1/2} = 0.30$ a.u.).

trum (electron yield versus excess energy). For a pulse of the form (3) the envelope field strength varies from zero to F_{peak} and back, and if an intermediate state shifts into resonance at a strength $F \leq F_{\text{peak}}$ (this happens two times during the pulse), the photoelectron yield will increase and one can observe a REMPI peak at the corresponding value of E_e .

The positions of REMPI peaks can be predicted using recently calculated data for resonant dynamic Stark shift for sodium [16] shown in Figure 4. One can see that for 760 nm laser radiation sodium states $4s$, $4f$, $5p$, $5f$ and $6p$ shift into resonance with an integer multiple of the laser frequency (2ω and 3ω) at different values of F , given in Table 1. Then, the energies related to REMPI peaks are obtained from equation (5) for these values of field strength.

The photoelectron spectra at three values of the field strength, obtained from the PMD are shown in Figure 5. The agreement between the values for E_e from Table 1 and the positions of maxima in the spectra confirms that the substructures (local maxima) in the main (non-resonant) four-photon-absorption maximum are related to the REMPI via corresponding intermediate states (2+2 REMPI via $4s$ state and 3+1 REMPI via $4f$, $5p$, $5f$, $6p$

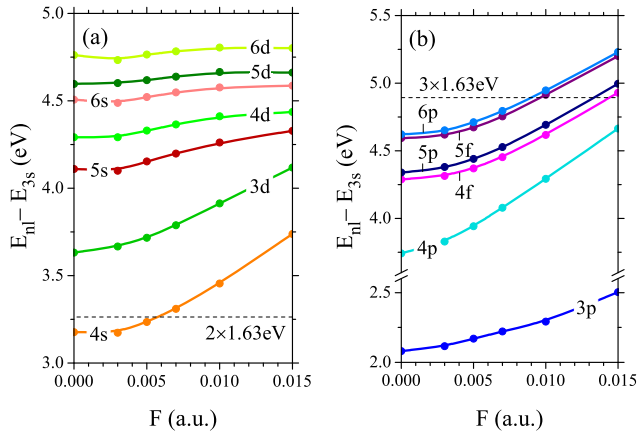


Fig. 4. The field-strength dependence of excited state energies E_{nl} relative to the ground state energy E_{3s} for the sodium atom in the laser field of frequency $\omega(F)$ under the K -photon resonance condition [$E_{nl}(\omega, F) - E_{3s}(\omega, F) = K\omega$]: (a) $K = 2$, (b) $K = 1$ (for $nl = 3p$) and $K = 3$ [16]. Horizontal dashed lines in parts (a) and (b) mark the two- and three-photon energies, respectively, for the laser field of 760 nm wave length.

Table 1. The values for laser field strength (electric component), laser intensity and photoelectron excess energy which characterize the resonant K -photon excitation of sodium states $4s$, $4f$, $5p$, $5f$ and $6p$ and subsequent ionization by 760 nm laser field ($\omega \approx 1.63$ eV).

Sate	K	F (a.u.)	Intensity (W/cm^2)	E_e (eV)
$4s$	2	0.0058	1.181×10^{12}	1.285
$4f$	3	0.0144	7.277×10^{12}	0.764
$5p$	3	0.0134	6.302×10^{12}	0.848
$5f$	3	0.0096	3.234×10^{12}	1.110
$6p$	3	0.0090	2.843×10^{12}	1.143

states). During the laser pulse with $F_{\text{peak}} = 0.007$ a.u. only $4s$ state transiently shifts into resonance (see Fig. 5a), but for the pulses with $F_{\text{peak}} = 0.01$ a.u. and $F_{\text{peak}} = 0.015$ a.u. this happens also with $5f$ and $6p$ states (Fig. 5b) and additionally with $4f$ and $5p$ states (Fig. 5c), respectively.

6 Summary

Multiphoton ionization of sodium by a femtosecond laser pulse of 760 nm wavelength and different peak intensities is studied by calculating the PAD, the PMD and the photoelectron energy spectra. The distributions are determined by applying the single-electron model, where the valence electron moves in an effective core potential and the external electromagnetic field, and calculating the evolution of the electron wave function until a time after the end of the pulse.

By inspecting the positions of maxima in the PAD and PMD, it is confirmed that s , d and g partial waves are emitted when four photons are absorbed, and p , f and h waves in the case of five-photon ionization (ATI). The g -wave is dominant in the former and the h -wave in the

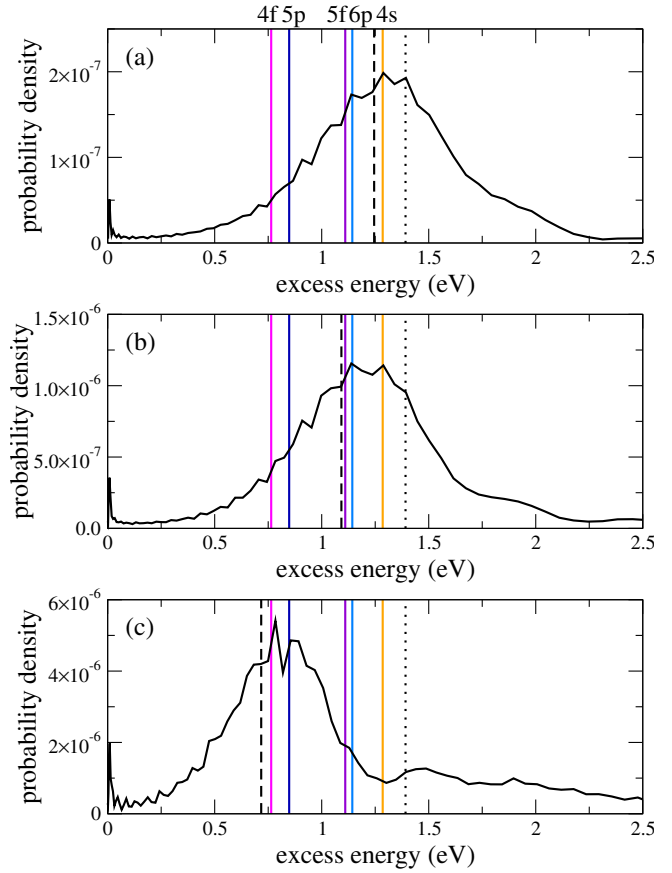


Fig. 5. Calculated photoelectron spectrum (probability density versus excess energy at $t = 1000$ a.u. – black line) of the sodium atom interacting with 10 fs laser pulse (3) with $\omega = 0.06$ a.u. (760 nm wavelength) and three peak values of the field strength: (a) $F_{\text{peak}} = 0.007$ a.u., (b) $F_{\text{peak}} = 0.01$ a.u. and (c) $F_{\text{peak}} = 0.015$ a.u. Substructures in the main maximum are related to the 2+2 REMPI via $4s$ state and 3+1 REMPI via $4f$, $5p$, $5f$ and $6p$ states. The corresponding values of photoelectron excess energies E_e estimated from the values of resonant dynamic Stark shift (see Fig. 4) and equation (5) are shown (vertical full lines). The weak-field value of the photoelectron excess energy at the non-resonant four-photon ionization ($E_e^{(0)} = 1.39$ eV), as well as those estimated using equation (5), are denoted by the dotted and dashed lines, respectively.

latter case. These facts indicate that the main photoabsorption pathway goes via F -states.

Using the resonant-dynamic-Stark-shift data for the sodium atom [16] it is shown that substructures observed in the main (nonresonant) maximum in the photoelectron spectra at the four-photon ionization of this atom are related to the REMPI via intermediate $4s$, $4f$, $5p$, $5f$ and $6p$ states.

This work was supported by the COST Action No. CM1204 (XLIC). We acknowledge support from the Ministry of Education, Science and Technological Development of Republic of Serbia under Project No. 171020.

Author contribution statement

All the authors were involved in the preparation of the manuscript. All the authors have read and approved the final manuscript.

References

1. M.H. Mittleman, *Introduction to the Theory of Laser-Atom Interactions* (Plenum Press, New York, 1982), p. 121
2. N.B. Delone, V.P. Krainov, *Multiphoton Processes in Atoms* (Springer, Heidelberg, 2000), Vol. 13
3. F. Grossmann, *Theoretical Femtosecond Physics* (Springer-Verlag, Berlin, 2008)
4. C.J. Joachain, N.J. Kylstra, R.M. Potvliege, *Atoms in Intense Laser Fields* (Cambridge University Press, Cambridge, 2012)
5. P. Agostini, F. Fabre, G. Mainfray, G. Petite, N.K. Rahman, *Phys. Rev. Lett.* **42**, 1127 (1979)
6. R.R. Freeman, P.H. Bucksbaum, H. Milchberg, S. Darack, D. Schumacher, M.E. Geusic, *Phys. Rev. Lett.* **59**, 1092 (1987)
7. M. Schuricke, G. Zhu, J. Steinmann, K. Simeonidis, I. Ivanov, A. Kheifets, A.N. Grum-Grzhimailo, K. Bartschat, A. Dorn, J. Ullrich, *Phys. Rev. A* **83**, 023413 (2011)
8. M. Krug, T. Bayer, M. Wollenhaupt, C. Sarpe-Tudoran, T. Baumert, S.S. Ivanov, N.V. Vitanov, *New J. Phys.* **11**, 105051 (2009)
9. N.A. Hart, J. Strohaber, A.A. Kolomenskii, G.G. Paulus, D. Bauer, H.A. Schuessler, *Phys. Rev. A* **93**, 063426 (2016)
10. H. Hellmann, *J. Chem. Phys.* **3**, 61 (1935)
11. M.Z. Milošević, N.S. Simonović, *Phys. Rev. A* **91**, 023424 (2015)
12. J.E. Sansonetti, *J. Phys. Chem. Ref. Data* **37**, 1659 (2008)
13. N.B. Delone, V.P. Krainov, *Physics – Uspekhi* **42**, 669 (1999)
14. J. Mitroy, M.S. Safronova, C.W. Clark, *J. Phys. B: At. Mol. Opt. Phys.* **43**, 202001 (2010)
15. A. Askar, A.S. Cakmak, *J. Chem. Phys.* **68**, 2794 (1978)
16. A. Bunjac, D.B. Popović, N.S. Simonović, to be published

CEPAS 2017

7th Conference on Elementary Processes in Atomic Systems



3rd – 6th September 2017

Průhonice, Czech Republic



Calculation of the dynamic Stark shift for sodium and the application to resonantly enhanced multiphoton ionization

A. Bunjac¹, D. B. Popović¹, N. S. Simonović¹

¹*Institute of Physics, University of Belgrade, P.O. Box 57, 11001 Belgrade, Serbia*

Although several monographs on the topic of the resonant dynamic Stark shift (RDSS) have been published [1, 2], accurate data in a wide range of parameters is still not available for most systems studied. A method for determining the RDSS, based on wave-packet calculations of the population probabilities of quantum states, is presented. It is almost insensitive to variations of the laser pulse profile, which ensures a generality in applications. The method is used to determine an RDSS data set for transitions $3s \rightarrow nl$ ($n \leq 6$) in sodium induced by the laser pulse with the peak intensities up to $7.9 \times 10^{12} \text{ W/cm}^2$ and wavelengths in the range from 455.6 to 1139 nm. The data is applied to analyze the photoelectron spectra (electron yield versus excess energy) of the sodium atom interacting with an 800 nm laser radiation. Substructures observed in the recent experimentally measured spectra [3] are successfully reproduced and related to the resonantly enhanced multiphoton ionization (REMPI) via specific (P and F) intermediate states.

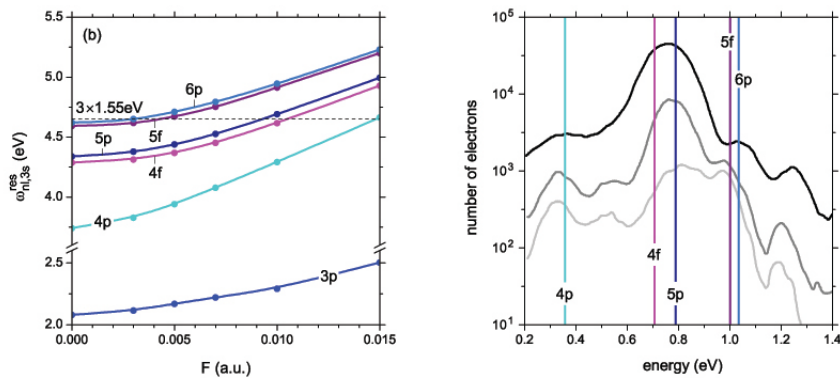
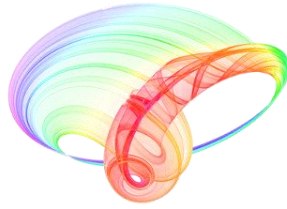


Figure 1: Left: The field-strength dependence of excited states energies relative to the ground state energy for the sodium atom in the laser field which is in K-photon resonance with transitions $3s \rightarrow nl$ $K = 1$ and $K = 3$. Horizontal dashed line marks the three-photon energy, for the laser field of 800 nm wavelength. Right: Calculated values for photoelectron excess energies (vertical lines) which characterize four-photon REMPI of sodium via 4p, 4f, 5p, 5f and 6p states by 800nm laser field, shown together with experimentally measured electron yield versus photoelectron excess energies obtained for 57 fs laser pulse with peak intensities $3.5 \times 10^{12} \text{ W/cm}^2$ (white gray, lower curve), $4.9 \times 10^{12} \text{ W/cm}^2$ (gray, middle curve), and $8.8 \times 10^{12} \text{ W/cm}^2$ (black, upper curve) [3].

- [1] N. B. Delone and V. P. Krainov, *Multiphoton Processes in Atoms*, Vol. 13, Springer, Heidelberg, 2000.
- [2] M. Fox, *Quantum Optics: An Introduction*, Oxford University Press, New York, 2006. p. 167.
- [3] N. A. Hart *et al.*, *Phys. Rev. A* **93** (2016) 063426.

Book of abstracts



PHOTONICA2017

The Sixth International School and Conference on Photonics

& COST actions: MP1406 and MP1402



&H2020-MSCA-RISE-2015 CARDIALLY workshop



28 August – 1 September 2017

Belgrade, Serbia

Editors

Marina Lekić and Aleksandar Krmpot

Institute of Physics Belgrade, Serbia

Belgrade, 2017

Calculation of populations of energy levels of sodium interacting with an intense laser pulse and estimation of the resonant dynamic Stark shift

A. Bunjac¹, D. B. Popović¹ and N. S. Simonović¹
Institute of Physics, University of Belgrade, Serbia
 e-mail:simonovic@ipb.ac.rs

Populations of energy levels of sodium interacting with a linearly polarized intense (up to 10^{13} W/cm²) laser pulse of a few femtoseconds duration with wavelengths in the visible and near infrared domain are determined by solving the time-dependent Schrödinger equation (TDSE) for the valence (active) electron which is considered as moving in an effective potential of the atomic core and the external electromagnetic field [1]. To solve the TDSE we used two different methods: (i) the method of time-dependent coefficients (TDC) and (ii) the wave-packet propagation (WPP) method. In the TDC method the total wave-function is expanded in a finite basis of unperturbed atomic (bound) states and their populations at the end of the pulse are determined from the values of expansion coefficients at that time. In the WPP method the total wave function is discretized on a coordinate grid and its evolution is calculated using the second-order-difference scheme [1, 2]. Compared to the TDC method the WPP method is more time-consuming but also more accurate because in this case there is no restriction to a finite basis and the continuum states are taken into account. For the TDC calculations here we used a basis set consisting of the lowest 14 sodium states (s, p, d, f states from 3s to 6d). It is found that the calculated populations of low lying levels as functions of the laser frequency ω agree well with the results obtained by the PPT method in the range of laser peak intensities up to few TW/cm². The peaks in the population of excited states (nl) occurring when $K\omega = \omega_{nl,3s} \equiv E_{nl}(F, \omega) - E_{3s}(F, \omega)$ (multi(K)-photon resonance condition) are used to determine the field strength dependence of the resonant dynamic Stark shift for separations of levels.

REFERENCES

- [1] A. Bunjac, D. B. Popović and N. Simonović, Eur. Phys. J. D (2017), accepted for publication.
- [2] A. Askar and A. S. Cakmak, J. Chem. Phys. 68, 2794 (1978).



28th Summer School and International Symposium on the Physics of Ionized Gases

Aug. 29 - Sep. 2, 2016, Belgrade, Serbia

CONTRIBUTED PAPERS

&

ABSTRACTS OF INVITED LECTURES,
TOPICAL INVITED LECTURES, PROGRESS REPORTS
AND WORKSHOP LECTURES

Editors:

Dragana Marić, Aleksandar Milosavljević,
Bratislav Obradović and Goran Poparić



University of Belgrade,
Faculty of Physics



Serbian Academy
of Sciences and Arts

PHOTOIONIZATION OF SODIUM BY A FEW FEMTOSECOND LASER PULSE – TIME-DEPENDENT ANALYSIS

A. Bunjac, D. B. Popović and N. S. Simonović

Institute of Physics, University of Belgrade, P.O. Box 57, 11001 Belgrade, Serbia

Abstract. Multiphoton ionization of sodium by a few femtosecond duration laser pulse is examined using the single-electron model where the valence electron moves in an effective core potential and the external electromagnetic field. The photoelectron angular and momentum distributions are studied by inspecting the evolution of the electron wave function until some time after the end of the pulse. The AC Stark shift of the lowest state is estimated and the appearance of the above threshold ionization is observed.

1. INTRODUCTION

Interaction of strong laser fields with atoms may lead to the photoionization of the later even when the single photon energy is lower than the ionization potential of atom. This process is known as the multiphoton ionization (MPI). Contrary to the single photon ionization, where the ionization rate is large even at very low intensities, the probability for multiphoton processes is much lower and they occur only at sufficiently strong fields. From the theoretical point of view this means that a perturbative treatment, that is a valid approach in describing the single photon ionization, usually fails when applying to MPI. A clear indication of the non-perturbative regime is the so-called above threshold ionization (ATI), in which the atom absorbs more photons than the minimum required. Here we study the MPI of the sodium atom in strong laser fields by solving numerically the time-dependent Schrödinger equation for this system within the single-electron approximation. A similar analysis has been recently done for lithium [1].

2. THE MODEL

Within the single-electron model and the frozen core approximation the dynamics of the valence (active) electron of sodium atom in an

alternating electric field $F(t)$ is described by Hamiltonian (in atomic units)

$$H = \frac{\mathbf{p}^2}{2} + V_{\text{core}}(r) - F(t)z. \quad (1)$$

The effective core potential (ECP) $V_{\text{core}}(r)$ describes the interaction of the valence electron with the atomic core (inner electrons + atomic nucleus). For this purpose we shall use the Hellmann's pseudopotential [2]

$$V_{\text{core}}(r) = -\frac{1}{r} + \frac{A}{r} e^{-ar}. \quad (2)$$

The parameters $A = 21$ and $a = 2.54920$ [3] provide the correct value for the ionization potential of sodium $I_p = 5.1391 \text{ eV} = 0.18886 \text{ a.u.}$ and reproduce approximately the energies of singly-excited states (see Fig. 1).

We consider the linearly polarized laser pulse of the form

$$F(t) = F_{\text{peak}} \sin^2(\pi t/T_p) \cos(\omega t), \quad 0 < t < T_p \quad (3)$$

(otherwise $F(t) = 0$). Here ω , F_{peak} and T_p are the frequency of laser field, the peak value of its electric component and the pulse duration, respectively. Due to the axial symmetry of the system the magnetic quantum number m of the valence electron is a good quantum number for any field strength. Since in the sodium ground state (when $F = 0$) the orbital and magnetic quantum numbers of this electron are equal zero, in calculations we choose $m = 0$.

3. THE METHOD

The photoionization process is simulated by calculating the evolution of the initial wave function $\psi(\mathbf{r}, 0)$, which is the lowest eigenstate of Hamiltonian (1) at $t = 0$ (then $F = 0$), until some time after the end of the pulse. This can be done by taking an adequate representation of the evolution operator $U(t, t + \Delta t)$ and integrating numerically the relation $\psi(\mathbf{r}, t + \Delta t) = U(t, t + \Delta t)\psi(\mathbf{r}, t)$ with a sufficiently small time step Δt . Here we use of the second-order-difference (SOD) scheme [4]

$$\psi(\mathbf{r}, t + \Delta t) = \psi(\mathbf{r}, t - \Delta t) - 2i\Delta t H \psi(\mathbf{r}, t) \quad (4)$$

that is for this purpose adapted to cylindrical coordinates. Due to the axial symmetry of the system described by the Hamiltonian (1) this observable as well as the electron's wave function do not depend on the azimuthal angle and the dynamics reduces to two degrees of freedom (ρ and z).

4. RESULTS

We study the photoionization of the sodium atom by a 760 nm ($\omega = 0.06 \text{ a.u.}$) laser pulse of the form (3) with the peak intensity $1.72 \times 10^{12} \text{ W/cm}^2$ ($F_{\text{peak}} = 0.007 \text{ a.u.}$) and 10 fs duration ($T_p = 413.4 \text{ a.u.}$).

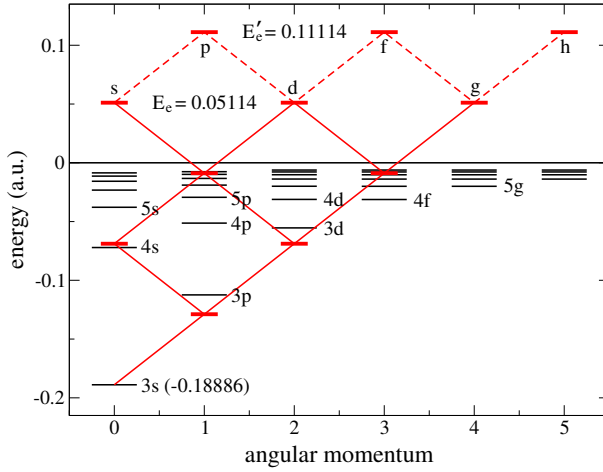


Figure 1. Energy scheme of sodium including the lowest excited states as well as possible four-photon and five-photon (ATI) absorption pathways ($\omega = 0.06$ a.u.) from the 3s ground state to the continuum.

The energy level diagram (Fig. 1) illustrates that from the ground state (3s) at least four photons with $\omega = 0.06$ are required to reach the continuum. Then, the excess energy of the photoelectrons is expected to be $E_e = 0.05114$ a.u.

The probability distribution $|\psi(\mathbf{r}, t)|^2$ of the active (valence) electron is shown in Fig. 2 at $t = 1000$ a.u. and $t = 1200$ a.u. The outgoing wave determines the photoelectron angular distribution. Apart from the strong emission along the laser polarization ($\vartheta = 0^\circ$ and 180°) the distribution shows also maxima at $\vartheta \approx 45^\circ$, $\vartheta = 90^\circ$ and $\vartheta \approx 135^\circ$. The observed distribution relates to a superposition of the accessible emitted partial waves. In the case of four-photon absorption s, d and g partial waves can be emitted

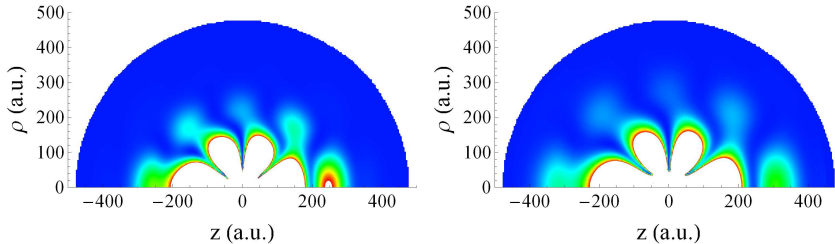


Figure 2. Probability distribution $|\psi(\mathbf{r}, t)|^2$ of the active electron of the sodium atom affected by the laser pulse (3) with $\omega = 0.06$ a.u. and $F = 0.007$ a.u. at: $t = 1000$ a.u. (left) and $t = 1200$ a.u. (right). The outgoing wave (with five maxima) determines the photoelectron angular distribution.

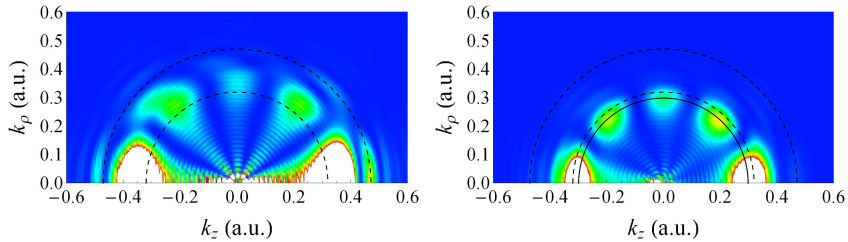


Figure 3. The photoelectron momentum distribution for the process shown in Fig. 1 at: $t = 800$ a.u. (left) and $t = 1000$ a.u. (right). Dashed semicircles denote the expected values of the momentum for the four-photon (MPI) and five-photon (ATI) processes at low laser intensities. The full semicircle corresponds to an average value of maxima in the calculated photoelectron momentum distribution at $t = 1000$ a.u.

(see Fig. 1). The maxima/minima structure of the outgoing wave in Fig. 2 indicate that in this case the g partial wave is dominant (four minima).

The photoelectron momentum distribution shows a similar angular structure, but the maxima are approximately located at semicircles of radius $k_e \equiv (2E_e)^{1/2} = 0.3198$ a.u. At shorter times after the ionization the photoelectrons momenta are larger than k_e (see Fig. 3(a)), but later they approach the asymptotic values (see Fig. 3(b)). The remaining difference can be attributed to the AC Stark shift.

Besides the regular MPI with four photons, in Fig. 3 the ATI structure related to the five-photon absorption can be observed. In the latter case, according to the energy level diagram in Fig. 1, the photoelectron excess energy in the weak field limit should be $E'_e = 0.05114$ a.u. ($k'_e = .4715$ a.u.) and p , f and h partial waves can be emitted. The ATI structure in Fig. 3 is indeed located near k'_e and contains five minima that is a feature of h waves.

Acknowledgements

This work was supported by the COST Action No. CM1204 (XLIC). We acknowledge support from the Ministry of Education, Science and Technological Development of Republic of Serbia under Project No. 171020.

REFERENCES

- [1] M. Schuricke et al, Phys. Rev. A **83**, 023413 (2011).
- [2] H. Hellmann, J. Chem. Phys. **3**, 61 (1935).
- [3] M. Z. Milošević and N. S. Simonović, Phys. Rev. A **91**, 023424 (2015).
- [4] A. Askar and A. S. Cakmak, J. Chem. Phys. **68**, 2794 (1978).

STRONG-FIELD IONIZATION OF SODIUM IN THE QUASISTATIC REGIME

A. Bunjac, D. B. Popović and N. S. Simonović

Institute of Physics, University of Belgrade, P.O. Box 57, 11001 Belgrade, Serbia

Abstract. Strong field ionization of sodium in the quasistatic regime is examined by studying the valence electron wave packet dynamics in the static electric field. The lowest state energies and ionization rates obtained by this method for different strengths of the applied field agree well with the results determined using other methods. It is shown that, if the Keldysh parameter is significantly lower than one (quasistatic regime), the probability of ionization by a laser pulse can be obtained from the static rates.

1. INTRODUCTION

When atom is irradiated by a sufficiently strong electromagnetic field the multiphoton ionization may occur although the single photon energy is lower than the ionization potential of this atom. If the field is, however, so strong that it is comparable to the atomic potential, it distorts the later forming a potential barrier through which the electron can tunnel. Finally, at extremely strong fields the barrier is suppressed below the energy of the atomic state and the so-called over-the-barrier ionization (OBI) occurs. The transition between multiphoton and tunnelling regimes is governed by the Keldysh parameter $\gamma = \omega (2I_p)^{1/2} / F$ [1], where ω , F and I_p are the frequency of electromagnetic field, the peak value of its electric component and the ionization potential of the atom (in atomic units). If $\gamma \gg 1$ (low-intensity/short-wavelength limit) the multiphoton ionization dominates, whereas for $\gamma \ll 1$ (high-intensity/long-wavelength limit) the tunnel ionization or OBI does.

Tunnel ionization is successfully described by the semiclassical theory due to Ammosov, Delone and Krainov (ADK) [2]. It is based on the quasistatic approximation which assumes that for $\gamma \ll 1$ the electric field changes slowly enough that the static tunnelling rate can be calculated for each instantaneous value of the field. Then the tunnelling rate for the alternating field can be obtained by averaging the static rates over the field

period. Here we present the results for ionization rates of the sodium atom in quasistatic field obtained by the wave-packet propagation method and compare them with the ADK values, as well as with the results obtained recently by the complex-rotation method [3]. Also we demonstrate that, if the Keldysh parameter is significantly lower than one, the probability of ionization by a laser pulse can be obtained from the static rates.

2. THE MODEL

The valence electron of alkali metal atoms can be considered as moving in an effective potential describing the interaction between this electron and the atomic core (inner electrons + atomic nucleus). The simplest effective core potential (ECP) applicable for these atoms is the Hellmann's pseudopotential [4]

$$V_{\text{core}}(r) = -\frac{1}{r} + \frac{A}{r} e^{-ar}. \quad (1)$$

(Atomic units are used throughout the text.) We shall for the sodium atom use the values $A = 21$ and $a = 2.54920$ from Ref. [3] which provide the correct value for the ionization potential $I_p = 5.1391 \text{ eV} = 0.18886 \text{ a.u.}$

Using this single-electron model we study the sodium atom under the influence of a quasistatic electric field F . Within the so-called frozen core approximation the dynamics of the valence electron is described by Hamiltonian

$$H = \frac{\mathbf{p}^2}{2} + V_{\text{core}}(r) - Fz. \quad (2)$$

The core potential and the external field form a potential barrier with the saddle point at the z -axis. Since the electron can tunnel through or escape over the barrier, the atom has a nonzero probability of ionizing for any field strength $F \neq 0$. Thus, all states of the system described by Hamiltonian (2) have a resonant character. We shall consider the resonance with the lowest energy that is characterized by the magnetic quantum number $m = 0$.

3. THE METHOD

The energy spectrum of Hamiltonian (2) (for static fields) can be obtained from the autocorrelation function $c(t) = \langle \psi(0) | \psi(t) \rangle$, where the initial state $|\psi(0)\rangle$ is the lowest eigenstate of Hamiltonian (2) when $F = 0$ and $|\psi(t)\rangle$ is the corresponding state at a later time t (then $F \neq 0$). The evolution of the lowest state is calculated using the so-called second-order-difference (SOD) method [5]. The eigenenergies of (2) appear as Lorentzian peaks in the power spectrum of the autocorrelation function $|\text{FT}[c(t)]|^2$, where $\text{FT}[c(t)]$ is the Fourier transform of $c(t)$. These peaks contain the information about the resonance positions E and widths Γ (i.e. decay rates $w = \Gamma/\hbar$).

The tunnelling rates determined numerically will be compared with those given by the ADK theory [2]. For alkali-metal atoms in the ground state one has $l = m = 0$ and the ADK formula (for static fields) reduces to

$$w = |C_{n^*0}|^2 I_p \left(\frac{2F_0}{F}\right)^{2n^*-1} e^{-\frac{2F_0}{3F}}, \quad (3)$$

where $n^* = (2I_p)^{-1/2}$, $F_0 = (2I_p)^{3/2}$, and $|C_{n^*0}|^2 = 2^{2n^*}/[n^* \Gamma(n^*+1) \Gamma(n^*)]$. Since for alkali metals the energy of the lowest state changes rapidly with F , the ADK rates can be significantly improved by applying the correction $I_p \rightarrow -E(F) = I_p - \Delta E(F)$ in (3), which accounts for the Stark shift $\Delta E(F)$ of the lowest energy level. For $F \ll 1$ this shift can be expanded in a series, giving

$$E(F) = E(0) + \Delta E(F) = -I_p - \frac{1}{2}\alpha F^2 - \frac{1}{24}\gamma F^4. \quad (4)$$

The dipole polarizability and the second dipole hyperpolarizability for sodium are $\alpha = 162.7 \pm 0.8$ and $\gamma = (9.56 \pm 0.48) \times 10^5$, respectively.

4. RESULTS

The lowest state energies and widths (ionization rates) for the sodium atom at different strengths of the applied static electric field calculated by the wave-packet method [7] are shown in Fig. 1, together with the values obtained recently by the complex-rotation method [3]. The results are in a good agreement in the considered field domain. The energies and rates estimated from the Stark shift expansion (4) and the ADK theory, respectively, agree well with the presented numerical values in the tunnelling regime.

We consider further the linearly polarized laser pulse of the form

$$F(t) = F_{\text{peak}} \sin^2(\pi t/T_p) \cos(2\pi t/T_c), \quad 0 < t < T_p \quad (5)$$

(otherwise $F(t) = 0$) and take $F_{\text{peak}} = 0.01$ a.u. We choose the optical cycle period $T_c = 1931$ a.u. ($\lambda = 14 \mu\text{m}$) that provides $\gamma = 0.2$ and the pulse duration $T_p = 4T_c$. The quasistatic rate $w(F(t))$ for this pulse, obtained using the corrected ADK formula (see Eq. (3) and the text below), is shown in Fig. 1(b). In Fig. 1(c) the corresponding (quasistatic) ionization probability

$$P_{\text{ion}}^{(\text{qs})}(t) = 1 - \exp\left[-\int_0^t w(F(t')) dt'\right] \quad (6)$$

is compared with the probability P_{ion} obtained by calculating the evolution of the time-dependent system [6] defined by Hamiltonian (2) with the alternating field $F(t)$ of the form (5). $P_{\text{ion}}^{(\text{qs})}(t)$ and $P_{\text{ion}}(t)$ approach each other whenever $F = 0$, allowing us to determine the ionization probability at $t = T_p$ from the static rates [7]. The difference between $P_{\text{ion}}(T_p)$ and $P_{\text{ion}}^{(\text{qs})}(T_p)$ in this example ($\gamma = 0.2$) is less than 1%, but it increases for larger values of γ .

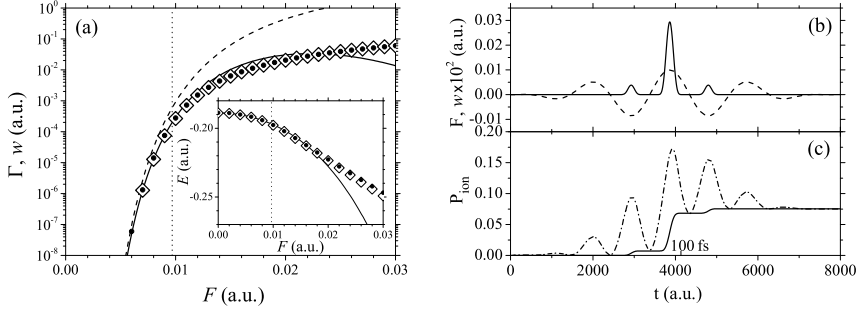


Figure 1. (a) Ionization rates of the sodium atom at different strengths of the static electric field F obtained by the wave-packet propagation method (full circles), by the complex-rotation method [3] (open 'diamonds'), by the ADK formula (3) (dashed line) and by the ADK formula with the Stark shift correction (4) (full line) are shown. The inset shows the numerical values for the lowest state energies (symbols) and those determined by the 4th order expansion formula (4) (full line). Vertical dotted lines mark the field strengths dividing the tunnelling and OBI areas (at $F = 0.00969$ for sodium). (b) The laser pulse of the form (5) with $F_{\text{peak}} = 0.01$ a.u., $T_c = 1931$ a.u., $T_p = 4T_c$ (dashed line) and the related quasistatic ionization rate $w(F(t))$ for sodium (full line). (c) The ionization probability obtained from the quasistatic rate (full line) and by solving the time-dependent problem exactly (dash-dot line).

Acknowledgements

This work was supported by the COST Action No. CM1204 (XLIC). We acknowledge support from the Ministry of Education, Science and Technological Development of Republic of Serbia under Project No. 171020.

REFERENCES

- [1] L. V. Keldysh, Sov. Phys. JETP **20**, 1307 (1965).
- [2] M. V. Ammosov, N. B. Delone, and V. P. Krainov, Sov. Phys. JETP **64**, 1191 (1986).
- [3] M. Z. Milošević and N. S. Simonović, Phys. Rev. A **91**, 023424 (2015).
- [4] H. Hellmann, J. Chem. Phys. **3**, 61 (1935).
- [5] A. Askar and A. S. Cakmak, J. Chem. Phys. **68**, 2794 (1978).
- [6] F. Grossmann, *Theoretical Femtosecond Physics* (Springer-Verlag, Berlin, 2008).
- [7] A. Bunjac, D. B. Popović, and N. S. Simonović, Eur. Phys. J. D **70**, 116 (2016).



Meeting of the XLIC Working Group 2

WG2 Expert Meeting on Biomolecules

27-30 April 2015, Fruška gora, Serbia



Institute of Physics Belgrade
University of Belgrade

Calculations of ionization probabilities for sodium in strong laser fields

A. Bunjac, D. B. Popović and N. Simonović

Institute of Physics, University of Belgrade, Pregrevica 118, Zemun, 11080 Belgrade

Ionization probabilities for sodium atom in strong laser fields are calculated for different ratios between the frequency and the field strength, covering both the quasistatic (tunneling/over-the-barrier) and the multiphoton ionization regimes. The probabilities are determined numerically using the wave-packet propagation technique [1] and the single electron model for alkali-metal atoms, where the valence electron moves in an effective core potential and the external field [2]. In the quasistatic regime (high-field-intensity/low-frequency) the ionization rate (probability per unit time) is obtained from the autocorrelation function, which is the overlap between the initial (here the ground) state $\psi(0)$ and the corresponding state $\psi(t)$ at a later time $t \geq 0$. The calculated values for the lowest state energies and ionization rates as functions of the field strength are in good agreement with the results obtained recently using other methods [2]. Additionally, the transition time from $t = 0$, when the external field is switched on, until the decaying (resonant) state becomes quasistationary (exponential decay) is estimated and the form of the final wave function is determined. The field ionization of sodium in the multiphoton regime (low-field-intensity/high-frequency) is studied for a linearly polarized laser pulse with the intensity profile of the electric field component $F \sin^2(\pi t/T_p)$ and the pulse duration T_p of a few femtoseconds. The ionization probability $P_{\text{ion}}(t)$ is determined by calculating the occupation probabilities $P_n(t)$ for each eigenstate of the valence electron as $P_{\text{ion}}(t) = 1 - \sum_n P_n(t)$ [3]. An example for the calculated probabilities as functions of time is shown in Fig. 1.

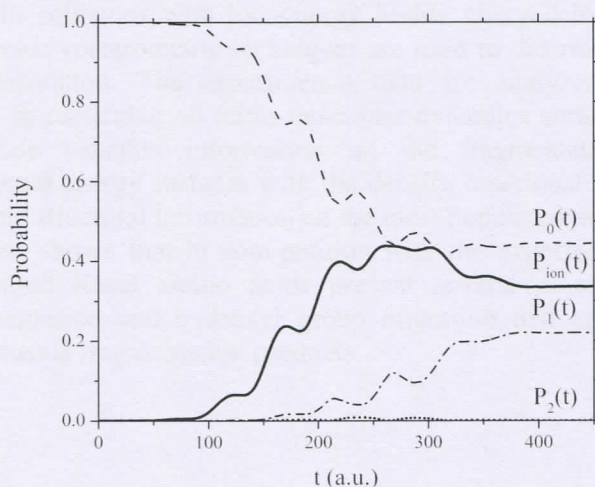


Fig.1. The occupation probabilities for the lowest three states as well as the related ionization probability for the sodium atom irradiated by the laser pulse of the wavelength $\lambda = 760$ nm, duration $T_p = 10$ fs (413.4 a.u.) and the peak intensity $1.72 \cdot 10^{12}$ W/cm² ($F = 0.007$ a.u.).

Acknowledgements: This work is supported by the COST Action No. CM1204 (XLIC). We acknowledge support from the Ministry of Education, Science and Technological Development of Republic of Serbia under Project No. 171020.

REFERENCES

- [1] M. D. Feit and J. A. Fleck, Jr., *J. Chem. Phys.* 78, 301 (1983).
- [2] M. Z. Milošević and N. S. Simonović, *Phys. Rev. A* 91, 023424 (2015).
- [3] F. Grossmann, *Theoretical Femtosecond Physics*, p. 106, (Springer, Berlin, 2008).

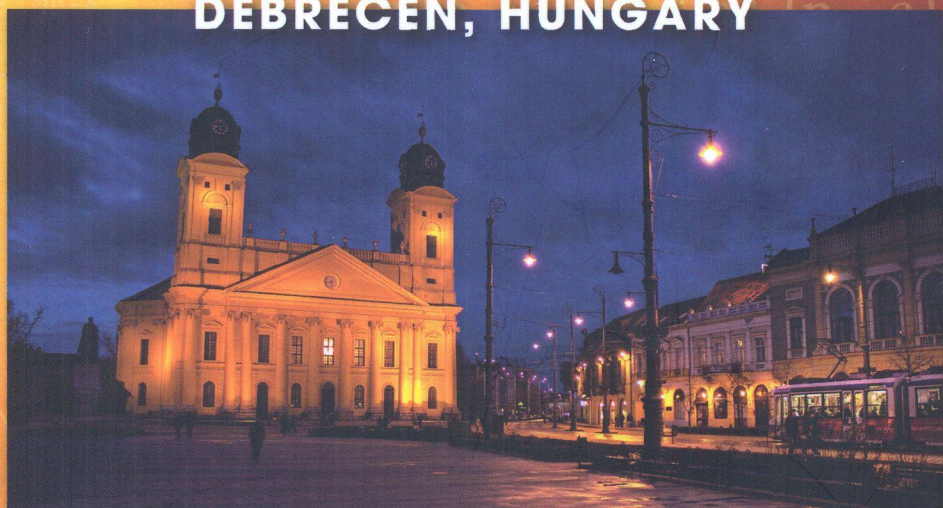
3rd
XLIC
XUV/X-ray light and fast
ions for ultrafast chemistry

GENERAL MEETING

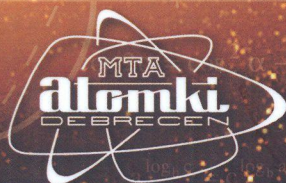
cost
EUROPEAN COOPERATION
IN SCIENCE AND TECHNOLOGY

(COST ACTION CM 1204)

**2-4 NOVEMBER 2015
DEBRECEN, HUNGARY**



PROGRAMME AND BOOK OF ABSTRACTS



3rd XLIC GENERAL MEETING
2-4 NOVEMBER, 2015

Organised by: *ATOMKI / DE / ELFT*

Venue

Centrum Hotel, Debrecen, Hungary

The conference will be hosted at Centrum Hotel, Debrecen, Hungary. The hotel is located in the very heart of the city, at 4-8 Kalvin square, next to the Reformed Great Church. All lectures, the poster sessions and the management committee meeting will be held here.

Book of Abstracts

This book contains the camera-ready copies of the abstracts as sent by the authors. In few cases only minor corrections were made.

Publisher: ATOMKI / DE / ELFT, Dr. Károly Tökési

Editor: Péter Badankó

Printed by: REXPO Kft., Manager: János Rác

ISBN: 978-963-8321-51-0

WELCOME

Welcome to the 3rd XLIC General Meeting XUV/X-ray light and fast ions for ultrafast chemistry (XLIC), organized in Debrecen (Hungary).

The workshop is an annual meeting of CM1204 action, which deals with physical and chemical phenomena induced by electromagnetic fields and charged particles. The meeting is planned for 2nd - 4th November, 2015. It will take place at Centrum Hotel, Debrecen, Hungary. There will be 24 talks given by invited speakers, 12 oral presentations by early stage scientists and 2 poster sessions.

The organization of this meeting and its funding with COST CM1204 budget was approved in the 3rd MC meeting, held in Gdansk (Poland) on October 10th, 2014.

The objectives of the workshop are to assess the state of the art in the current understanding of a variety of basic phenomena in the electron and atom dynamics such as charge-exchange processes collective as well as single-particle excitation and ionization, energy loss, and photon emission processes, collision induced physical, chemical and biological reactions radiation damage and materials modification.

The XLIC conference is held for the 3rd time. Previous conferences were organized in Madrid (Spain, 2013), Gdansk (Poland, 2014). It is a great honour for Debrecen to be the host of this prestigious event in 2015.

Debrecen is the second largest city of Hungary, one of the most important educational, research and cultural centres in Middle-Europe. Stadiums of Debrecen have given place to great sport events (like European Championship of Swimming, 2012) and the Carnival of Flowers attracts thousands of visitors from all over Europe every year. In addition, there are a lot of sights that must be seen, for instance the Great Church at the beautiful main square, Déri Museum, Reformed College and its unique library, the Great Forest and the main building of the University of Debrecen, but we could continue this list.

The 3rd XLIC conference is held at the Centrum Hotel. The hotel is located in the historic city centre of Debrecen, only 50 meters from the Great Reformed Church and the main square, the venue of many cultural events, in the close vicinity of the most important attractions, office buildings and institutions. It is one of the hotels of Eastern Hungary that provides ideal conditions for the work and recreation of business travellers, while also satisfying the needs of tourists in search of a lively atmosphere and vibrant experiences.

We hope that all participants will have a lively and successful meeting while enjoying the attractive surroundings in this beautiful region of Hungary. We hope, furthermore, we may offer exciting scientific programs in addition to various social and cultural programs, where you can enjoy the famous Hungarian dishes and wine, too. Organizers have been doing their best to guarantee pleasant experiences for everyone.

Károly Tőkési
Chair
3rd XLIC General Meeting

András Csehi
Co-Chair
3rd XLIC General Meeting

Calculation of probabilities and photoelectron angular distributions for strong field ionization of sodium

A. Bunjac^{1*}, D. B. Popović¹ and N. Simonović¹

¹Institute of Physics, University of Belgrade, Pregrevica 118, Zemun, 11080 Belgrade, Serbia

*Corresponding author: bunjac@ipb.ac.rs

Single ionization of the sodium atom in strong laser fields is studied for different frequencies and field strengths within the multiphoton ionization regime. The probabilities and photoelectron angular distributions are determined numerically using the wave-packet propagation technique [1] and the single electron model for alkali-metal atoms, where the valence electron moves in an effective core potential and the external field [2]. We considered a linearly polarized laser pulse with the intensity profile of the electric field component $F \sin^2(\pi t/T_p)$ and the pulse duration T_p of a few femtoseconds. The ionization probability $P_{\text{ion}}(t)$ is determined by calculating the occupation probabilities $P_n(t)$ for each eigenstate of the valence electron as $P_{\text{ion}}(t) = 1 - \sum_n P_n(t)$ (see e.g. Ref. 3). The photoelectron angular distributions are studied by inspecting the evolution of the electron wave function $\psi(\mathbf{r}, t)$ in the interval $(0, T_p)$. Examples for the calculated occupation and ionization probabilities as functions of frequencies at a given field strength, as well as the probability distribution of photoelectrons $|\psi(\mathbf{r}, t)|^2$ at a time near T_p are shown in Fig. 1. It is found that, due to low ionization potentials for alkali metal atoms, at the peak intensity of the laser field $\approx 3 \times 10^{12}$ W/cm² and wavelengths $\lambda \ll 3$ μm , the classical over-the-barrier threshold was reached inside the multiphoton regime.

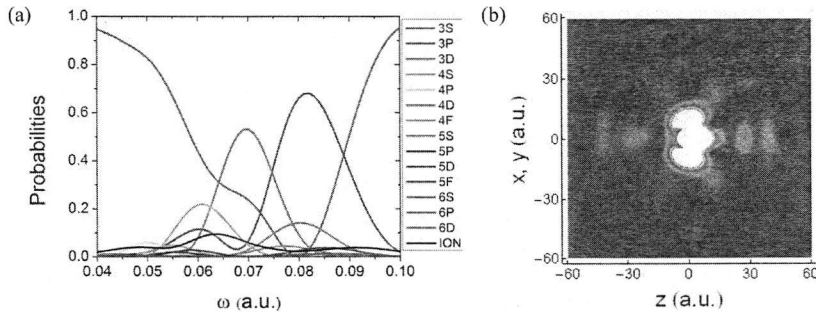


Figure 1: (a) Eigenstates occupation probabilities (different color lines) and the ionization probability (black line) as functions of the laser frequency ω at the peak intensity $1.72 \cdot 10^{12}$ W/cm² ($F = 0.007$ a.u.) at $t = T_p = 10$ fs. (b) The valence electron probability distribution $|\psi(\mathbf{r}, t)|^2$ at $t \approx T_p$ (for $\omega = 0.06$ a.u. and $F = 0.007$ a.u.). The outgoing wave determines the photoelectron angular distribution.

Acknowledgments: This work is supported by the COST Action No. CM1204 (XLIC). We acknowledge support from the Ministry of Education, Science and Technological Development of Republic of Serbia under Project No. 171020.

References

- [1] A. Askar and A. S. Cakmak, *J. Chem. Phys.*, **68**, 2794, (1978)
- [2] M. Z. Milošević and N. S. Simonović, *Phys. Rev. A*, **91**, 023424, (2015)
- [3] F. Grossmann, *Theoretical Femtosecond Physics* (Springer, Berlin, 2008), 106.